Discovery of a Novel Multitarget Analgesic Through an In Vivo-guided Approach

Guo Zhen , Nayeon Do , Nguyen Van Manh , Hee-Jin Ha , Hee Kim , Hyunsoo Kim , Kwanghyun Choi , Jihyae Ann * , Jeewoo Lee *

Posted Date: 27 December 2024

doi: 10.20944/preprints202412.2383.v1

Keywords: Novel analgesic; Multitarget analgesic; In vivo-guided approach

 doi:10.20944/preprints202412.2383.v1

Article

Discovery of a Novel Multitarget Analgesic Through an In Vivo-Guided Approach

Guo Zhen [1], Nayeon Do [1], Nguyen Van Manh [1], Hee-Jin Ha [2], Hee Kim [2], Hyunsoo Kim [2], Kwanghyun Choi [2], Jihyae Ann [1,*] and Jeewoo Lee [1,*]

[1] College of Pharmacy, Seoul National University, Seoul 08826, Republic of Korea

[2] Medifron DBT, Seoul 08502, Republic of Korea

* Correspondence: jihuya@snu.ac.kr (J.A.) jeewoo@snu.ac.kr (J.L.)

Abstract: Pain is a multifaceted condition influenced by peripheral, central, immune, and psychological factors. Targeting multiple pathways provides a holistic approach, enhancing efficacy, minimizing side effects, and reducing tolerance compared to single-target drugs. This study utilized an in vivo-guided approach to discover a novel multitarget analgesic, identifying compound **29** from a new scaffold (3) inspired by the pharmacophores of opiranserin and vilazodone. Analog screening in the formalin test identified compound **29** as a lead candidate for further study. Compound **29** demonstrated high potency in the formalin model, with an ED_{50} of 0.78 mg/kg in the second phase and a concentration-dependent trend in the first phase. In the spinal nerve ligation (SNL) neuropathic pain model, it exhibited dose-dependent analgesic effects, increasing withdrawal thresholds by 24% and 45% maximum possible effect (MPE) at 50 and 100 mg/kg, respectively. Mechanistic studies revealed that its analgesic activity is primarily driven by strong triple uptake inhibition, particularly at DAT and SERT, combined with high-affinity 5-HT_{2A} receptor antagonism. Pharmacokinetic studies in rats showed intraperitoneal administration provided a 5-fold increase in exposure and a 2-fold improvement in stability compared to oral administration. It also displayed high blood-brain barrier permeability, indicating suitability for CNS drugs. In vitro, compound **29** was nontoxic to HT-22 cells but exhibited potential hERG inhibition and strong CYP3A4 inhibition with minimal effects on other isozymes. In conclusions, compound **29** is a potent, multitarget analgesic discovered through an in vivo-guided approach. Ongoing optimization aims to mitigate side effects and further enhance its therapeutic profile.

Keywords: novel analgesic; multitarget analgesic; in vivo-guided approach

1. Introduction

Pain is a complex and multifactorial experience influenced by a combination of peripheral and central mechanisms, immune responses, and psychological factors [1]. This complexity presents a major challenge for the development of effective analgesic therapies, particularly for chronic and neuropathic pain conditions, which are often refractory to conventional treatments. Traditional single-target drugs, such as nonsteroidal anti-inflammatory drugs (NSAIDs) and opioids, have provided relief for some patients but are frequently associated with significant side effects, including tolerance, dependence, and limited efficacy in addressing the multiple dimensions of pain signaling.

In recent years, a shift toward multitarget approaches has gained momentum in drug discovery. By simultaneously modulating multiple pathways involved in pain transmission and modulation [2–4], multitarget analgesics offer a more comprehensive strategy that holds promise for better therapeutic outcomes [5–7]. This strategy has the potential to enhance efficacy, reduce side effects, and mitigate the risk of tolerance that commonly arises with single-target drugs.

One promising approach to discovering novel multitarget analgesics is the use of in vivo-guided models, which allow for the real-time evaluation of drug candidates in biological systems that closely

 doi:10.20944/preprints202412.2383.v1

mimic human pain pathways [8–10]. In vivo models provide invaluable insights into the pharmacodynamics and pharmacokinetics of compounds, enabling the identification of promising drug candidates that engage multiple targets relevant to pain.

In this study, we utilized an in vivo-guided approach to identify a novel multitarget analgesic that modulates key mechanisms involved in pain perception, transmission, and modulation. Through the integration of in vivo pain models and pharmacological assays, we aimed to discover and characterize a compound that addresses the limitations of current analgesics and offers potential as a more effective treatment for chronic and neuropathic pain.

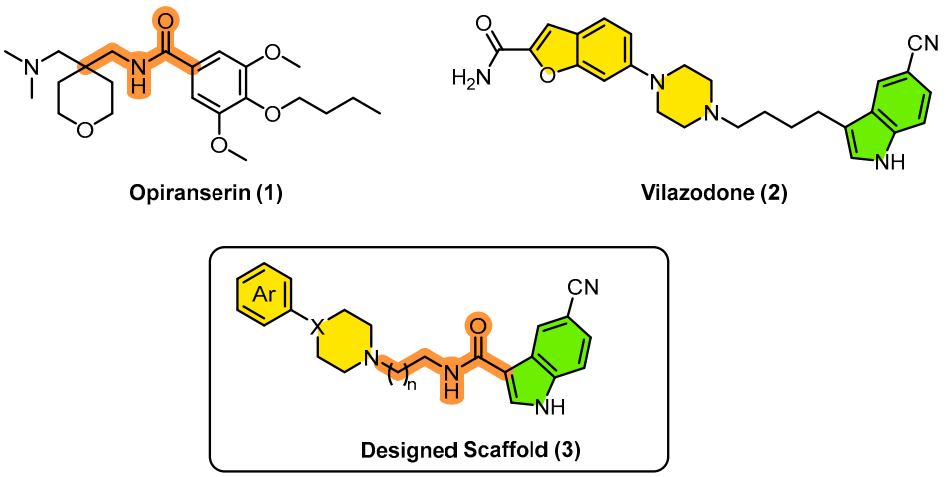

Figure 1. Newly designed scaffold based on the lead compounds.

Opiranserin (**1**), also known as VVZ-149, is a multitarget analgesic identified through ex-vivo screening [5]. This compound exhibits a unique pharmacological profile by selectively targeting several key pathways implicated in pain modulation. It functions as a glycine transporter 2 (GlyT2) blocker with an IC_{50} = 0.86 uM, effectively inhibiting the reuptake of glycine, a critical inhibitory neurotransmitter involved in spinal pain processing. Additionally, it acts as a purine receptor $P2X_3$ antagonist with an IC_{50} = 0.87 uM, targeting receptor associated with nociceptive signaling in peripheral sensory neurons. Furthermore, it demonstrates antagonistic activity at the serotonin receptor 5-HT_{2A} with an IC_{50} = 1.3 uM, modulating central serotonin pathways that contribute to pain perception. This multitarget profile makes opiranserin a promising candidate for managing diverse pain types, offering an alternative to traditional analgesics. Opiranserin has been studied clinically for intravenous use in the management of postoperative pain, aiming to reduce the need for opioid [11]. The drug was approved on December 2024 by the Ministry of Food and Drug Safety in Korea for the short-term treatment of moderate and severe acute postoperative pain in adults.

Vilazodone (**2**), primarily known as an antidepressant due to its dual action as a selective serotonin reuptake inhibitor (SSRI) and a partial agonist of the serotonin 5-HT_{1A} receptor, has shown potential as our lead compound in analgesic development [12,13]. Its mechanism of action, which modulates serotonin pathways, is relevant in pain perception and modulation. Serotonin plays a key role in descending pain pathways, which are involved in pain inhibition. By enhancing serotonin levels and activating 5-HT_{1A} receptors, vilazodone may help alleviate pain, particularly in conditions where central sensitization and neuropathic pain are involved. Additionally, its dual action reduces the likelihood of developing side effects commonly associated with traditional analgesics. Therefore, vilazodone represents a promising candidate for the development of novel analgesics targeting pain-related pathways.

As a primary *in-vivo* screening method, we employed the formalin test, a widely used experimental model in pain research, particularly for assessing the efficacy of potential analgesic

 doi:10.20944/preprints202412.2383.v1

candidates [14–18]. It involves injecting formalin into the paw of an animal, which induces a biphasic pain response—initial acute pain (1st phase) followed by a prolonged inflammatory phase (2nd phase). This biphasic response allows researchers to evaluate analgesics that target both **acute** (nociceptive) and **chronic** (inflammatory/neuropathic) pain mechanisms, offering insights into the multitarget potential of a compound. Since the test engages both peripheral nociceptor activation and central sensitization mechanisms, it enables the screening of compounds that may work at multiple levels of the pain pathway. Analgesics that reduce both the first and second phases of the formalin test could be considered as targeting both **peripheral and central pain mechanisms.** Given the complexity of the pain response in the formalin test, it is an ideal model for assessing multitarget analgesics. A novel analgesic may show efficacy in modulating both inflammatory and neuropathic components of pain, thus having broader therapeutic potential.

In our efforts to discover a novel multitarget analgesic through in vivo-guided screening, we designed a new scaffold (**3**) inspired by the pharmacophores of opiranserin and vilazodone. This design integrates a 5-cyanoindole core and either arylpiperazine or arylpiperidine, both of which are well-known 5-HT receptor modulators. These components are connected via an alkylamido linker, enabling dual functionality [19].

In this study, a series of scaffold **3** analogs was synthesized and subsequently screened for their ability to inhibit the 2nd phase of the formalin test, a key model for assessing analgesic potential. Among the synthesized compounds, compound **29** emerged as the lead condidate due to its significant inhibitory activity. This compound was selected for further in-depth investigation, including studies in a neuropathic pain model, detailed mechanism of action analyses, and comprehensive pharmacokinetic and toxicological evaluations.

2. Results and Discussion

2.1. Synthesis

For the synthesis of 4-aryl-1-aminoalkylpiperazine (Scheme 1), 1-arylpiperazine **7**, a key intermediate, was prepared using three distinct methods. First, an aniline-type aryl **4** was reacted directly with bis(2-chloroethyl)amine hydrochloride to produce piperazine **7**. Second, aromatic halides **5** undewent palladium-catalyzed coupling with *N*-Boc-piperazine, followed by Boc group deprotection, yielding **7**. Third, a 2-chloropyridine-type aryl **6** was directly condensed with piperazine to obtain **7**. Subsequent alkylation of **7** with (*N*-Boc)-aminoethyl iodide or (*N*-Boc)-aminopropyl bromide produced intermediate **8**, which, upon Boc group deprotection, yielded 1-aryl-4-aminoalkylpiperidine **11**.

Conversely, 4-aryl-1-aminoalkylpiperidine **12** was synthesized starting from commercially available 4-arylpiperidine **9**, following the same synthetic pathway employed for the corresponding piperazine analogs.

For the synthesis of 4-arylcarbonyl-1-aminoalkylpiperazine (Scheme 2), aromatic acyl halide **13** was condensed with *N*-Boc-piperazine to form an intermediate **14**, which, after Boc deprotection, yielded **15**. Alkylation of **15** with (*N*-Boc)-aminoalkyl halide, followed by subsequent deprotection provided the primary amines **17**.

The final compounds (**20**-**55**) were synthesized by coupling the amines, **11**, **12**, and **17**, with either 5-cyano-1H-indole-3-carboxylic acid **18** or its *N*-Boc protected analog **19**, using 1-ethyl-3-(3-dimethylaminopropyl)carbodiimide (EDC) as the coupling reagent, respectively (Scheme 3). This synthetic strategy enabled the generation of a diverse library of compounds for pharmacological evaluation.

Preprints.org (www.preprints.org) | NOT PEER-REVIEWED | Posted: 27 December 2024 doi:10.20944/preprints202412.2383.v1

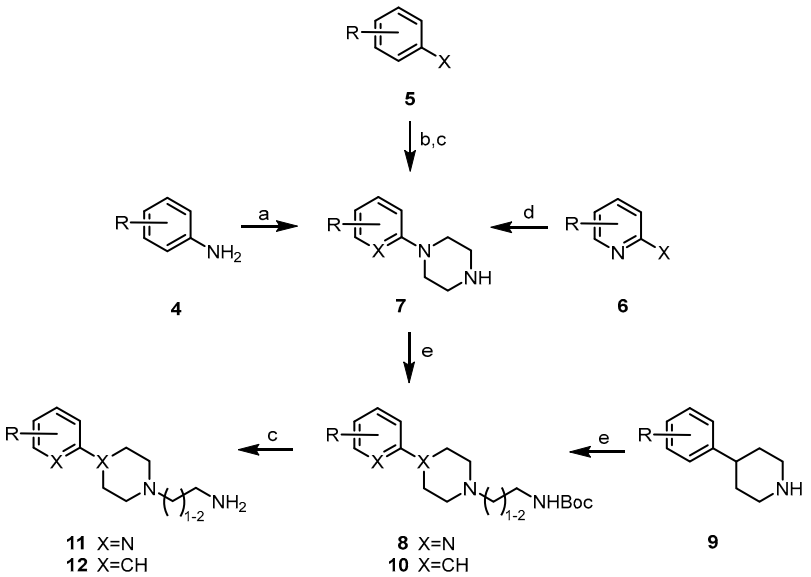

Scheme 1. Synthesis of 4-aryl-1-aminoalkylpiperazine/piperidine analogs. **Reagents and conditions**: (a) [Method A] HCl·NH(CH_2CH_2Cl)$_2$, 1,2-dichlorobenzene, 180 °C, 2 h: [Method B] HCl·NH(CH_2CH_2Cl)$_2$, ethylene glycol monomethyl ether, 150 °C, overnight; (b) *N*-Boc-piperazine, Pd(dba)$_3$, NaOtBu, BINAP, toluene, reflux, overnight; (c) CF_3CO_2H, CH_2Cl_2, r.t., 1 h; (d) piperazine, ethylene glycol, 140 °C, 2 h; (e) I(CH_2)$_2$NHBoc or Br(CH_2)$_3$NHBoc, CH_3CN, 60 °C, overnight.

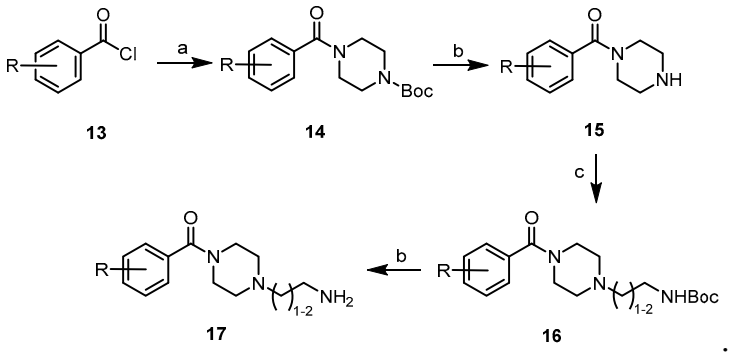

Scheme 2. Synthesis of 4-arylcarbonyl-1-aminoalkylpiperazine. **Reagents and conditions**: (a) *N*-Boc-piperazine, NEt_3, CH_2Cl_2, r.t., 3 h; (b) CF_3CO_2H, CH_2Cl_2, r.t., 1 h; (c) I(CH_2)$_2$NHBoc or Br(CH_2)$_3$NHBoc, CH_3CN, 60 °C, overnight.

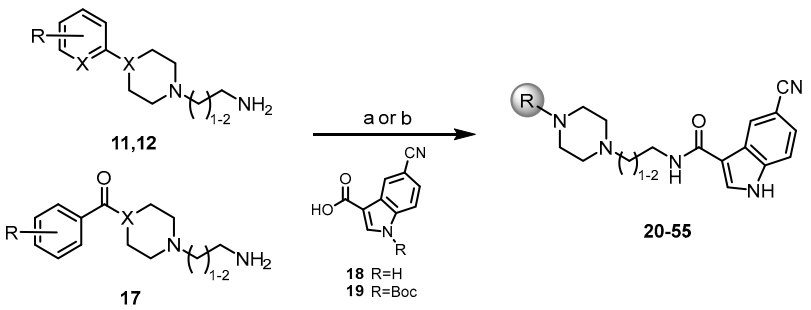

Scheme 3. Synthesis of the final compounds. **Reagents and conditions**: (a) **18**, EDC, HOBt, DIPEA, CH_2C1_2, r.t., overnight; (b) i) **19**, EDC, HOBt, DIPEA, CH_2C1_2, r.t., overnight, ii) CF_3CO_2H, CH_2Cl_2, r.t., 6 h.

 doi:10.20944/preprints202412.2383.v1

2.2. Animal studies

2.2.1. Primary In Vivo Screening

For primary screening, the synthesized compounds were administered to mice via intraperitoneal injection at a dose of 5 mg/kg using the formalin model. The percentage inhibition relative to the vehicle in the second phase was calculated, and the results are presented in Tables 1 and 2.

The structure-activity relationship (SAR) analysis provided valuable insights. In the series of piperazine analogs, the ethyl linker derivatives generally demonstrated greater inhibition compared to the corresponding propyl linker derivatives (Table 1). Within the aryl ring series, the 3-substituted phenyl analogs (**20**-**22**, **36**-**38**) exhibited superior inhibitory activity compared to the corresponding 4-substituted analogs (**23**-**25**, **39**-**41**). Notably, 3-chlorophenyl analogs, **21** and **37**, as well as the 3-trifluoromethyl analog **22**, showed exceptional inhibition in this test. In contrast, the pyridine analogs (**26**-**28**, **42**-**44**) displayed moderate inhibitory activity.

Further investigation into various bicyclic aryl groups commonly utilized in 5-HT modulating CNS drugs revealed additional trends. Examples include quinoline (**29**, **45**) as seen in quipazine; 2-carbamoylbenzofuran (**30**, **46**) as in vilazodone; (2,4-dimethylphenyl)thiophenyl (**31**, **47**) as in vortioxetine; benzisothiazole (**32**, **48**) as in ziprasidone. Among these, only quinoline analogs, **29** and **45**, demonstrated strong inhibition in both ethyl and propyl linkers. Additionally, arylcarbonyl analogs (**33**-**35**, **49**-**51**), including 2,3-dihydrobenzo[1,4]dioxine-2-carbonyl group as in doxazosin, exhibited weak to moderate inhibitory activity.

In the series of piperidine analogs, derivatives such as 6-fluorobenzoisoxazole (**52**, **54**) as in risperidone, and 6-chlorobenzimidazol-2-one (**53**, **55**) as in clopimozide, were explored at the 4-position of piperdine. These compounds also displayed weak to moderate inhibitory activity (Table 2).

Overall, six compounds, 3-chlorophenyl (**21** and **37**), 3-trifluorophenyl (**22**), quinoline (**29** and **45**), (2,4-dimethylphenyl)thiophenyl (**31**) derivatives, exhibited inhibition percentages exceeding 70% among the 36 compounds tested. These compounds were selected for further evaluation to determine their ED_{50} values in the formalin model.

Table 1. 5-Cyano-*N*-(2-(4-arylpiperazin-1-yl)ethyl/propyl)-indole-3-carboxamide analogs.

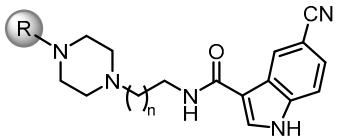

R	n=1	% Inhibition	n=2	% Inhibition
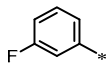	**20**	3.1	**36**	NE
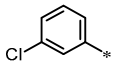	**21**	90.6	**37**	81.4
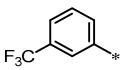	**22**	94.6	**38**	37.1
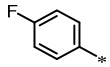	**23**	35.8	**39**	NE
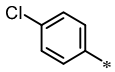	**24**	1.6	**40**	4.7
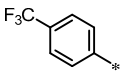	**25**	19.8	**41**	16.5

Preprints.org (www.preprints.org) | NOT PEER-REVIEWED | Posted: 27 December 2024 doi:10.20944/preprints202412.2383.v1

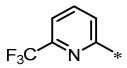	**26**	48.6	**42**	45.7
	**27**	48.0	**43**	45.3
	**28**	NE	**44**	3.7
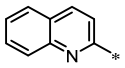	**29**	98	**45**	96.5
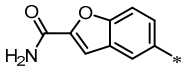	**30**	23.8	**46**	49.2
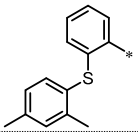	**31**	75.0	**47**	NE
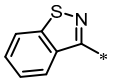	**32**	14.3	**48**	NE
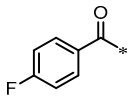	**33**	24.2	**49**	20.3
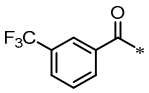	**34**	2.1	**50**	2.9
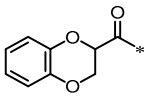	**35**	0.4	**51**	27.3

Table 2. 5-Cyano-*N*-2(3)-(4-arylpiperidin-1-yl)ethyl(propyl)-indole-3-carboamide.

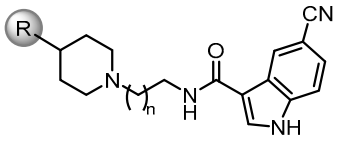

R	n=1	% Inhibition	n=2	% Inhibition
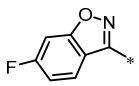	**52**	46.7	**54**	NE
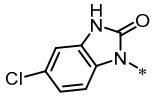	**53**	14.3	**55**	24.0

2.2.2. Formalin MODEL Study

The six selected compounds, which demonstrated strong inhibitory effects exceeding 70% during initial screenings, was further evaluated to determine their ED_{50} values in the 2nd phase of the formalin model. Each compound was assessed using four doses (0.1, 1, 5 and 10 mg/kg) by intraperitoneal injection.

All tested compounds exhibited potent analgesic effects, with ED_{50} values ranging from 0.79 to 3.2 mg/kg in the 2nd phase of the model. Among them, compound **29** demonstrated the highest

 doi:10.20944/preprints202412.2383.v1

potency, with an ED_{50} value of 0.78 mg/kg, indicating its superior efficacy compared to the other compounds (Table 3). While the activity of the compound in the 1st phase was relatively weak, a trend of concentration-dependent inhibition was observed during this phase (Figure 2). This finding suggests that compound **29** may exert its effects through mechanisms that are more prominent in the later, inflammatory phase of the formalin model. Such results underscore the compound's potential as a highly effective analgesic agent with both dose-dependent and phase-specific activity.

Table 3. ED_{50} values of the selected compounds in the formalin model.

Compound	% Inhibition	ED_{50}
21	90.6	2.3
22	94.6	1.3
29	98	0.78
31	75	2.66
37	81.4	3.2
45	96.5	0.93

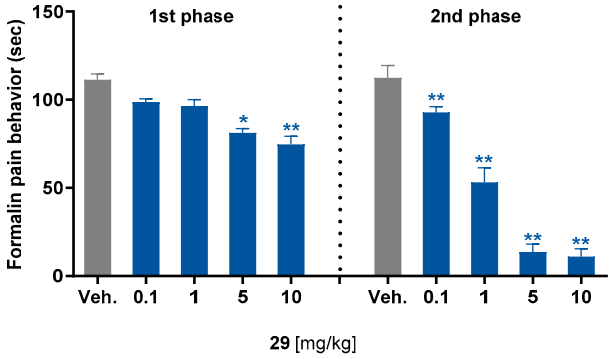

Figure 2. Analgesic activity of compound **29** in the formalin model. Results are expressed as mean ± SEM (n = 8). *p < 0.05, **p < 0.01 compared to the vehicle, based on one-way analysis of variance (ANOVA), followed by Bonferroni's post hoc test.

2.2.3. Neuropathic Pain Model Study

To evaluate its potency in neuropathic pain, compound **29** was tested in the **spinal nerve ligation (SNL) model,** a representative model for neuropathic pain [20,21].

The **SNL model, also known as the Chung model,** is a widely used animal model for studying **neuropathic pain**, a chronic pain condition resulting from nervous system damage. This model replicates human neuropathic pain, which can stem from nerve injuries due to conditions like diabetes, shingles, or spinal cord injury. In the SNL model, the L5 or L6 spinal nerve is surgically ligated to induce nerve injury, leading to the development of long-lasting neuropathic pain symptoms in the animal. Following the nerve injury, animals display pain-related behaviors that mirror those seen in human neuropathic pain conditions, such as **allodynia** and **hyperalgesia.** Behavioral assessments conducted on 14 days after surgery evaluate the animal's sensitivity to mechanical stimuli using Von Frey filaments to quantify pain responses and measure mechanical allodynia.

In this experiment, compound **29** was administered intraperitoneally at two different doses, 50 and 100 mg/kg, and its analgesic effects were assessed by measuring the 50% withdrawal threshold at multiple time points (1, 3 and 5 hours post-administration) (Figure 3A). Compound **29** demonstrated dose-dependent analgesic activity, as evidenced by an increase in the withdrawal

 doi:10.20944/preprints202412.2383.v1

threshold. The analgesic effect was most pronounced at 3 hours after administration, indicating a T_{max} of 3 hours, as confirmed by an *in vivo* pharmacokinetic study (refer to Figure 4 and Table 6). At this peak, the compound achieved a maximum possible effect (MPE) of 24% at the 50 mg/kg dose and 45% at the 100 mg/kg dose (Figure 3B). These results clearly highlight the compound's ability to produce significant analgesic effects in a dose-dependent manner in a neuropathic pain model, with a notable enhancement in efficacy observed at the higher dose.

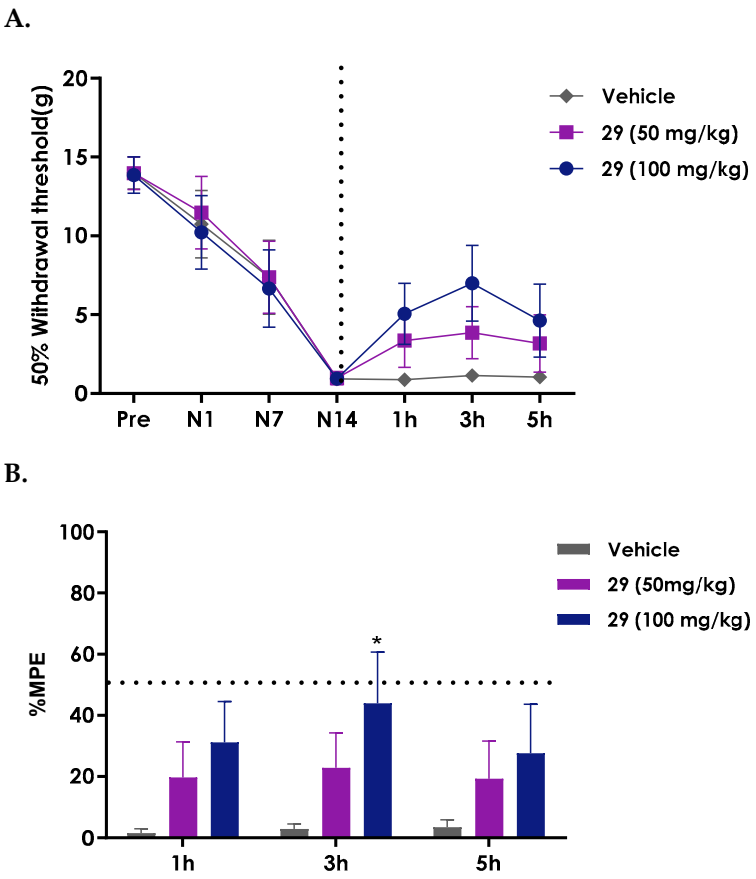

Figure 3. Antinociceptive effect of compound **29** in the SNL model in rats. (A) The mechanical allodynia was induced using von Frey filaments and was expressed as 50% of paw withdrawal before surgery and at 1, 7 and 14 days after nerve ligation (N1, N7, and N14) and at 1, 3 and 5 hrs after administration of vehicle or chemical at 50 and 100 mg/kg. The dotted line represents the beginning of the treatment with test compound. (B) The antinociceptive activity of 50 and 100 mg/kg of compound 29 at 1, 3 and 5 hrs after administration was expressed as percentage of maximum possible effect (MPE). The data are expressed as the means ± SEM. Statistical analysis using Student's t-test: *$p < 0.05$ compared to the vehicle-treated group.

2.3. Mechanism Study

To elucidate the mechanism of action of compound **29** in producing analgesic effects, its inhibitory effects were systematically evaluated through a screening process. The compound was tested at a concentration of 10 μM against a diverse panel of 47 drug target molecules that are closely associated with pain modulation pathways. The results indicated that, among them, 16 targets exhibited more than 50% inhibition in response to compound **29**. This suggests that the compound interacts significantly with a subset of targets involved in pain signaling. To further refine these findings and understand the potency of its activity, IC_{50} values were subsequently determined for those receptors, compared to their corresponding representative reference, demonstrating the highest levels of inhibition among the 16 identified targets (Table 4).

Compound **29** demonstrated strong inhibition of monoamine reuptake at dopamine (DAT), norepinephrine (NET) and serotonin (SERT) transporters, with K_i values of 0.046, 0.38 and 0.13 μM,

 doi:10.20944/preprints202412.2383.v1

respectively. These values indicate that it was 19 times more potent than at DAT compared to vanoxerine, 3 times more potent at NET compared to desipramine, and 13 times more potent at SERT compared to fluoxetine, highlighting compound 29's superior efficacy in modulating monoamine transporter activity compared to these widely known reference compounds.

Additionally, compound **29** exhibited notable binding affinity for several key receptor associated with pain modulation and neurotransmitter systems. Specifically it showed binding affinities for the adrenergic α_{2A} receptor, dopamine D_{2L} (long isoform of D_2 receptor) and serotonin 5-HT_{2A} receptor, with K_i values of 4.11, 1.85 and 0.15 mM, respectively. These values correspond to 0.25, 0.02, and 1.53 times the activity of reference compounds, yohimbine, spiperone and ketanserin, respectively, highlighting the compound's broad interaction with neurotransmitter system.

Overall, the analgesic mechanism of compound **29** is primarily attributed to its strong triple monoamine uptake inhibition, with a particularly potent effect observed at DAT and SERT. Additionally its activity at the 5-HT_{2A} receptor further supports its potential as a multifaceted agent in pain management. The combined activity across these targets underscores the compound's promise as a therapeutic candidate with diverse and complementary mechanism of action.

Table 4. IC_{50} values of compound **29** for the receptors with the highest potency.

	IC_{50} (μM)	K_i (μM)	n_H[a]
Transporter, Dopamine (DAT)			
Vanoxerine	1.08	0.86	1.01
29	0.057	0.046	0.88
Transporter, Norepinephrine (NET)			
Desipramine	1.09	1.08	0.84
29	0.38	0.38	0.73
Transporter, Serotonin (SERT)			
Fluoxetine	10.1	1.64	0.74
29	0.78	0.13	0.84
Adrenergic α_{2A}			
Yohimbine	2.08	1.04	0.88
29	8.22	4.11	1.02
Dopamine D_{2L}			
Spiperone	0.12	0.041	0.71
29	5.54	1.85	0.86
Serotonin 5-HT_{2A}			
Ketanserin	0.81	0.23	0.99
29	0.52	0.15	0.88

[a] n_H : Hill coefficient, n=1 non-cooperative.

2.4. Pharmacokinetic Study

In the *in vitro* metabolic stability study, the stability of compound **29** was evaluated using liver microsomes derived from both mouse and human sources. The primary objectives of this study was to determine the metabolic clearance rate of compound **29** over a defined time period, enabling an assessment of its intrinsic clearance. Microsomal incubations were performed, and the percentage of intact compound remaining was quantified at specific time points.

After 30 minutes of incubation, it was observed that 51.2% of the parent compound remained intact in mouse liver microsomes, while 55.6% remained intact in human liver microsomes (Table 5). These results suggest that compound **29** demonstrates moderate metabolic stability across both species, with slightly higher stability in human microsomes compared to mouse microsomes. Such findings are indicative of the compound's potential for further investigation in drug development.

To assess the ability of compound **29** to permeate the **blood-brain barrier (BBB)**, a BBB PAMPA (Parallel Artificial Membrane Permeability Assay) experiment was conducted. This assay is a widely used in vitro model to predict the potential of compounds to cross the BBB. During the experiment, the permeability of compound **29** was quantified by measuring its LogPe value, which was

 doi:10.20944/preprints202412.2383.v1

determined to be 4.5 (Table 5). This high value strongly indicates that it has a high potential to permeate the BBB efficiently. With its high BBB permeability, compound **29** is expected to exert pharmacological effects in the brain, making it a promising candidate for central nervous system (CNS) drugs.

Table 5. *In vitro* pharmacokinetic profile of compound **29**.

Metabolic stability[a]	51.2% (mouse), 55.6% (human)
BBB PAMPA	Log Pe = 4.5

[a] % remaining for 30 min.

The *in vivo* pharmacokinetics parameters of compound **29** were measured in rats over 24 h following intraperitoneal (ip) and oral (po) administration (Figure 4). These experiments were conducted to evaluate the compound's absorption, distribution, metabolism, and excretion profiles under different routes of administration.

Following ip administration at a dose of 5 mg/kg, the mean area under the curve from the time of dosing to the last measurable concentration (AUC_{last}) was 1,030 ng·h/mL, with a maximum plasma concentration (C_{max}) of 208 ng/mL. The half-life of the compound under this route of administration was calculaed to be 3.49 hours, with a time to reach maximum concentration (T_{max}) of 2.83 hours. These results suggests a relatively high systemic exposure and sustained plasma concentration following ip administration. In contrast, oral administration at a dose of 10 mg/kg resulted in an AUC_{last} of 407 ng·h/mL and a C_{max} of 113 ng/mL. The half-life was significantly shorter at 1.67 hours, and the T_{max} was observed to be 1.50 hours. Compared to ip administration, the oral route showed approximately 5-fold lower exposure and 2-fold lower *in vivo* stability (Table 6).

These findings highlight the pharmacokinetic advantages of ip administration for animal studies of compound **29**, demonstrating greater systemic exposure and prolonged stability compared to oral administration.

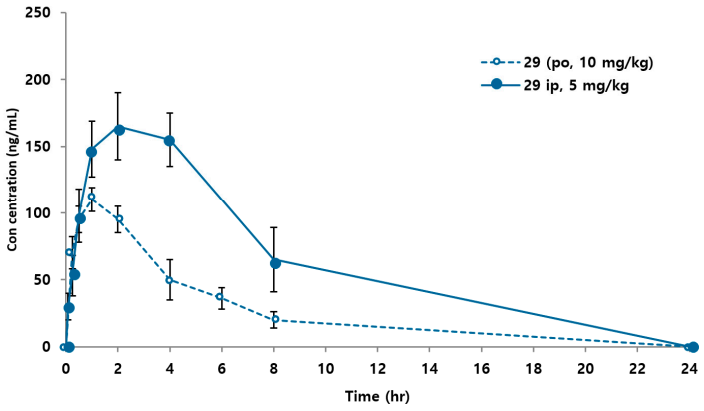

Figure 4. Mean plasma concentration-time profile of compound **29** following intraperitoneal and oral administration in Sprague–Dawley rats.

Table 6. Pharmacokinetics parameters of compound **29** following intraperitoneal and oral administration in Sprague–Dawley rats.

PK Parameters	Unit	IP	PO
Dose	mg/kg	5	10
AUC_{last}	ng·h/mL	1030	407
AUC_{inf}	ng·h/mL	1381	430
C_{max}	ng/mL	208	113
T_{max}	h	2.83	1.50
Cl/F	L/h/kg	3.88	24.04

 doi:10.20944/preprints202412.2383.v1

V_d	L/kg	17.9	57.4
$t_{1/2}$	h	3.49	1.67

2.5. Toxicity Study

In the *in vitro* toxicity study, we initially evaluated the cytotoxic potential of compound **29** using a hippocampal neuronal cell line (HT-22), a commonly used model for assessing neurotoxicity. Cell viability was determined after exposure to compound **29** at a concentration of 10 μM. The result indicated that it did not exhibit any toxic effects on HT-22 cells, as cell viability was maintained at levels exceeding 100% relative to the untreated control group. These findings suggest that compound **29** is nontoxic at the tested concentration, supporting its potential for further development and use in biological systems without significant cytotoxicity concerns.

The **hERG gene** encodes a cardiac potassium ion channel (Kv11.1) that is critical for the repolarization phase of the cardiac action potential. This channel plays a pivotal role in returning ventricular muscle cells to their resting state following depolarization. Inhibition or suppression of hERG channel activity by a drug can lead to a prolonged action potential duration, increasing the risk of cardiac arrhythmias such as ventricular fibrillation and the potentially fatal condition torsades de pointes.

To evaluate the cardiotoxicity of compound **29**, a **hERG fluorescence polarization assay** was conducted, with results compared to E-4031, a well-known and potent hERG channel inhibitor used as a positive reference. At a concentration of 10 μM, it exhibited 52.7% inhibition of hERG channel activity. Based on this degree of inhibition, its IC_{50} value was estimated to be approximately 10 μM (**Table 7**). These findings indicate that compound **29** has a moderate potential for hERG channel inhibition, which warrants further investigation to assess its cardiotoxic risk in clinical applications.

Table 7. hERG inhibition of compound **29**.

FP assay	Inhibition %[a]
29	52.7
E-4031	100

[a] % of inhibition at 10 μM.

In the drug–drug interaction study, the potential inhibitory effects of compound **29** on cytochrome P450 (CYP) enzymes were assessed by examining five representative isozymes: CYP1A2, CYP3A4, CYP2C9, CYP2C19, and CYP2D6. Ketoconazole, a well-characterized strong inhibitor of CYP3A4, was used as the reference inhibitor to validate the assay conditions. At a tested concentration of 10 μM, compound **29** exhibited minimal inhibitory activity (less than 50% inhibition) against CYP1A2, CYP2C9, CYP2C19, and CYP2D6, indicating that a low likelihood of significant interactions with these enzymes. However, it demonstrated substantial inhibition of CYP3A4, the most abundant isozyme, with 78% activity suppression under the same conditions. This level of inhibition suggests that compound **29** is a strong CYP3A4 inhibitor, which may have implications for its potential drug-drug interaction profile. (Table 8).

Table 8. CYP isozyme inhibition of compound **29**.

	CYP1A2	**CYP3A4**	**CYP2C9**	**CYP2C19**	**CYP2D6**
24[a]	0	78	47	43	11
Ketoconazole[b]	0	68	3.2	0	0

[a] % of inhibition at 10 μM. [b] CYP3A4 inhibitor (IC_{50} = 0.1 μM).

 doi:10.20944/preprints202412.2383.v1

3. Materials and Methods

3.1. Chemistry

All chemical reagents and solvents were commercially available. Silica gel column chromatography was performed using ZEOprep 60/40–63 μm silica gel (ZEOCHEM, Louisville, KY, USA). 1H and 13C NMR spectra were recorded on JEOL JNM-ECZ400S spectrrometer (400 MHz for 1H and 100 MHz for 13C; JEOL Ltd., Akishima, Tokyo, Japan).

Chemical shifts are reported in parts per million (ppm) relative to tetramethylsilane (Me_4Si) as internal standard. High-resolution mass spectra (HRMS) were measured by fast atom bombardment (FAB) with a JEOL JMS-700 MStation instrument (JEOL Ltd., Akishima, Tokyo, Japan). All final compounds were purified to greater than 95% purity, as determined by high-performance liquid chromatography (HPLC). HPLC was performed on an Agilent 1120 Compact LC (G4288A) instrument (Agilent Technologies, Santaclara, CA, USA) using an Agilent TC-C18 column (4.6 mm × 250 mm, 5 μm).

General Procedure

3.1.1. Synthesis of 1-arylpiperazine 7 (Procedure 1)

Method A:

A mixture of aniline-type aryl **4** (1.0 equiv) and bis-(2-chloroethyl)amine hydrochloride (1.2 equiv) in 1,2-dichlorobenzene was stirred at 180°C for 2h or in ethylene glycol and monomethyl ether was stirred at 150°C for overnight. After completion, the reaction mixture was cooled to room temperature, diluted with water, and extracted twice with ethyl acetate (EtOAc). The organic phase was collected, washed thrice with water, dried over $MgSO_4$, and concentrated under vacuum. The residue was purified using silica gel column chromatography with MeOH/MC (1:20 and 1:10) as an eluent to afford the desired product **7**.

Method B, C:

A solution of aromatic halides **5** (1.0 equiv) in Toluene was added with NaOtBu (2 equiv), $Pd(dba)_3$ (0.025 equiv), BINAP (0.05 equiv) and *N*-Boc-piperazine (1.0 equiv) was reflux overnight. After completion, the reaction mixture was cooled to room temperature, diluted with water, and extracted twice with ethyl acetate (EtOAc). The organic phase was collected, washed thrice with water, dried over $MgSO_4$, and concentrated under vacuum. The residue was purified using silica gel column chromatography with MeOH/MC (1:20 and 1:10) as an eluent to afford the Boc-piperazine intermediate. Then the intermediate (1.0 equiv) dissolved in MC was added with TFA (10 equiv) at 0°C and stirred at room temperature for 1h. After completion, the reaction mixture was neutralized with 1N NaOH to PH > 7 at 0°C, diluted with water, and extracted twice with MC and ethyl acetate (EtOAc). The organic phase was collected, dried over $MgSO_4$, and concentrated under vacuum to afford the desired product **7**.

Method D:

A mixture of 2-chloropyridine-type aryl **6** (1.0 equiv) and piperazine (10 equiv) in ethylene glycol was stirred at 140°C for 2h. After completion, the reaction mixture was cooled to room temperature, diluted with water, and extracted twice with ethyl acetate (EtOAc). The organic phase was collected, washed thrice with water, dried over $MgSO_4$, and concentrated under vacuum. The residue was purified using silica gel column chromatography with MeOH/MC (1:20 and 1:10) as an eluent to afford the desired product **7**.

3.1.2. Alkylation of 7 or 9 or 15 (Procedure 2)

A solution of 1-arylpiperazine **7** or commercially available 4-arylpiperidine **9** or intermediate **15** (1.0 equiv) in ACN was added with (*N*-Boc)-aminoethyl iodide or (*N*-Boc)-aminopropyl bromide (1.5 equiv) and K_2CO_3 (2 equiv) and stirred at 60°C overnight. After completion, the reaction mixture was cooled to room temperature, filtrated to remove the K_2CO_3, washed with MC and concentrated under

 doi:10.20944/preprints202412.2383.v1

vacuum. Then purified using silica gel column chromatography with MeOH/MC (1:40) as an eluent to afford the desired productm **8** or **10** or **16** .

3.1.3. Deprotection of 8 or 10 or 14 or 16 (Procedure 3)

A solution of intermediate **8** or **10** or **14** or **16** (1.0 equiv) in MC was added with TFA (10 equiv) at 0°C and stirred at room temperature for 1h. After completion, the reaction mixture was neutralized with 1N NaOH to PH>7 at 0°C, diluted with water, and extracted twice with MC and ethyl acetate (EtOAc). The organic phase was collected, dried over $MgSO_4$, and concentrated under vacuum to afford the desired product **11** or **12** or **15** or **17**.

3.1.4. Synthesis of 14 (Procedure 4)

A mixture of aromatic acyl halide **13** (1.0 equiv) in MC was added with *N*-Boc-piperazine (1.0 equiv) and TEA (2 equiv) at 0°C and stirred at room temperature for 3h. After completion, the reaction mixture was diluted with water, and extracted twice with MC. The organic phase was collected, dried over $MgSO_4$, and concentrated under vacuum. The residue was purified using silica gel column chromatography with EtOAc/hexane (1:7 and 1:4) as an eluent to afford the desired product **14**.

3.1.5. EDC Coupling (Procedure 5)

A mixture of 5-cyano-1H-indole-3-carboxylic acid **18** or its *N*-Boc protected analog **19** (0.9 equiv) in MC was added with HOBt (1.5 equiv) , EDC (1.5 equiv) and DIPEA (3 equiv) at 0°C and stirred at 0°C for 30min. And then added the amine **11** or **12** or **17** (1.0 equiv) and stirred at room temperature for overnight. After completion, the reaction mixture was diluted with water, and extracted twice with MC and ethyl acetate (EtOAc). The organic phase was collected, dried over $MgSO_4$, and concentrated under vacuum. The residue was purified using silica gel column chromatography with MeOH/MC (1:20) as an eluent to afford the desired product **20-55**.

5-Cyano-N-(2-(4-(3-fluorophenyl)piperazin-1-yl)ethyl)-1H-indole-3-carboxamide (20)

Yield 55%, white solid, mp: 225.8 °C; ^{1}H NMR (500 MHz, DMSO-d_6) δ 12.01 (s, 1H), 8.46-8.54 (m, 1H), 8.15-8.22 (m, 1H), 7.96-8.02 (m, 1H), 7.57-7.63 (m, 1H), 7.42-7.51 (m, 1H), 7.06-7.18 (m, 1H), 6.66-6.74 (m, 2H), 6.47-6.54 (m, 1H), 3.40 (q, J = 6.6 Hz, 2H), 3.13-3.15 (m, 4H), 2.53-2.59 (m, 4H), 2.50 (t, J = 6.9 Hz, 2H); ^{13}C NMR (500 MHz, DMSO-d_6) δ 164.93, 164.19, 162.86, 153.38, 153.31, 138.40, 130.83, 130.75, 130.62, 126.83, 126.35, 125.13, 120.96, 113.91, 111.96, 111.31, 111.29, 105.15, 104.99, 103.13, 102.28, 102.08, 57.77, 53.13, 48.20, 36.67; HRMS (FAB) calc. for $C_{22}H_{22}FN_5O$, $[M+H]^+$: 392.1887, found: 392.1898.

N-(2-(4-(3-Chlorophenyl)piperazin-1-yl)ethyl)-5-cyano-1H-indole-3-carboxamide (21)

Yield 50%, white solid, mp: 218.2 °C; ^{1}H NMR (500 MHz, DMSO-d_6) δ 12.01 (s, 1H), 8.51-8.63 (m, 1H), 8.14-8.17 (m, 1H), 7.96-8.02 (m, 1H), 7.57-7.71 (m, 1H), 7.45-7.51 (m, 1H), 7.13-7.20 (m, 1H), 6.87-6.98 (m, 1H), 6.84-6.86 (m, 1H), 6.72-6.76 (m, 1H), 3.37-3.47 (m, 2H), 3.10-3.20 (m, 4H), 2.53-2.60 (m, 4H), 2.50 (t, J = 7.1 Hz, 2H); ^{13}C NMR (500 MHz, DMSO-d_6) δ 164.19, 152.80, 138.40, 134.32, 130.91, 130.63, 126.83, 126.36, 125.13, 120.97, 118.47, 114.99, 114.12, 113.91, 111.96, 103.13, 57.77, 53.14, 48.19, 36.67; HRMS (FAB) calc. for $C_{22}H_{22}ClN_5O$, $[M+H]^+$: 408.1591, found: 408.1596.

5-Cyano-N-(2-(4-(3-(trifluoromethyl)phenyl)piperazin-1-yl)ethyl)-1H-indole-3-carboxamide (22)

Yield 17%, white solid, mp: 214.7 °C; ^{1}H NMR (500 MHz, DMSO-d_6) δ 12.03 (s, 1H), 8.51 (t, J = 0.8 Hz, 1H), 8.14 (s, 1H), 8.01 (t, J = 5.7 Hz, 1H), 7.58 (dd, J = 8.5, 0.6 Hz, 1H), 7.47 (dd, J = 8.5, 1.6 Hz, 1H), 7.37 (t, J = 8.0 Hz, 1H), 7.18 (d, J = 8.5 Hz, 1H), 7.12 (s, 1H), 7.02 (d, J = 7.5 Hz, 1H), 3.40 (q, J = 6.5 Hz, 2H), 3.20 (t, J = 5.0 Hz, 4H), 2.56-2.60 (m, 4H), 2.51 (t, J = 6.9 Hz, 2H); ^{13}C NMR (500 MHz, DMSO-d_6) δ 164.19, 151.77, 138.34, 130.63, 130.50, 130.47, 126.82, 126.35, 126.06, 125.13, 120.96, 119.09, 115.00, 113.97, 111.96, 111.16, 103.12, 57.75, 53.13, 48.14, 36.57; HRMS (FAB) calc. for $C_{23}H_{22}F_3N_5O$, $[M+H]^+$: 442.1855, found: 442.1848.

5-Cyano-N-(2-(4-(4-fluorophenyl)piperazin-1-yl)ethyl)-1H-indole-3-carboxamide (23)

 doi:10.20944/preprints202412.2383.v1

Yield 68%, white solid, mp: 222.6 °C; ^{1}H NMR (500 MHz, DMSO-*d*$_6$) δ 11.90-12.02 (m, 1H), 8.47-8.54 (m, 1H), 8.10-8.17 (m, 1H), 7.96-8.02 (m, 1H), 7.55-7.60 (m, 1H), 7.44-7.50 (m, 1H), 6.96-7.04 (m, 2H), 6.83-6.93 (m, 2H), 3.39 (q, J = 6.6 Hz, 2H), 3.00-3.05 (m, 4H), 2.55-2.60 (m, 4H), 2.50 (t, J = 6.9 Hz, 2H); ^{13}C NMR (500 MHz, DMSO-*d*$_6$) δ 164.22, 157.41, 155.54, 148.48, 138.40, 130.62, 126.82, 126.34, 125.14, 120.97, 117.59, 117.53, 115.83, 115.65, 113.91, 111.96, 103.13, 57.77, 53.31, 49.51, 36.67; HRMS (FAB) calc. for $C_{22}H_{22}FN_5O$, $[M+H]^+$: 392.1887, found: 392.1883.

N-(2-(4-(4-Chlorophenyl)piperazin-1-yl)ethyl)-5-cyano-1H-indole-3-carboxamide (24)

Yield 71%, white solid, mp: 252.1 °C; ^{1}H NMR (500 MHz, DMSO-*d*$_6$) δ 12.02 (s, 1H), 8.47-8.55 (m, 1H), 8.14 (s, 1H), 8.01 (t, J = 5.8 Hz, 1H), 7.54-7.60 (m, 1H), 7.41-7.49 (m, 1H), 7.13-7.21 (m, 2H), 6.85-6.96 (m, 2H), 3.39 (q, J = 6.5 Hz, 2H), 3.05-3.10 (m, 4H), 2.55 (t, J = 5.0 Hz, 4H), 2.50 (t, J = 7.1 Hz, 2H); ^{13}C NMR (500 MHz, DMSO-*d*$_6$) δ 164.22, 150.37, 138.40, 130.62, 129.10, 126.82, 126.34, 125.14, 122.76, 120.97, 117.29, 113.91, 111.95, 103.13, 57.76, 53.15, 48.54, 36.66; HRMS (FAB) calc. for $C_{22}H_{22}ClN_5O$, $[M+H]^+$: 408.1591, found: 408.1596.

5-Cyano-N-(2-(4-(4-(trifluoromethyl)phenyl)piperazin-1-yl)ethyl)-1H-indole-3-carboxamide (25)

Yield 62%, white solid, mp: 250.9 °C; ^{1}H NMR (500 MHz, DMSO-*d*$_6$) δ 12.02 (s, 1H), 8.51 (q, J = 0.7 Hz, 1H), 8.16 (d, J = 15.1 Hz, 1H), 7.96-8.02 (m, 1H), 7.53-7.59 (m, 1H), 7.44-7.48 (m, 3H), 7.01 (d, J = 8.8 Hz, 2H), 3.40 (q, J = 6.5 Hz, 2H), 3.21-3.26 (m, 4H), 2.54-2.60 (m, 4H), 2.51 (t, J = 6.9 Hz, 2H); ^{13}C NMR (500 MHz, DMSO-*d*$_6$) δ 164.20, 153.81, 138.40, 130.63, 126.83, 126.68, 126.64, 126.61, 126.36, 125.13, 120.96, 118.15, 114.63, 113.91, 111.96, 103.13, 57.76, 53.02, 47.53, 36.66; HRMS (FAB) calc. for $C_{23}H_{22}F_3N_5O$, $[M+H]^+$: 442.1855, found: 442.1848.

5-Cyano-N-(2-(4-(6-(trifluoromethyl)pyridin-2-yl)piperazin-1-yl)ethyl)-1H-indole-3-carboxamide (26)

Yield 67%, white solid, mp: 231.3 °C; ^{1}H NMR (500 MHz, DMSO-*d*$_6$) δ 12.02 (s, 1H), 8.51-8.54 (m, 1H), 8.17 (d, J = 14.4 Hz, 1H), 7.96-8.03 (m, 1H), 7.63-7.71 (m, 1H), 7.55-7.60 (m, 1H), 7.42-7.51 (m, 1H), 7.07-7.11 (m, 1H), 7.00 (q, J = 7.2 Hz, 1H), 3.52 (t, J = 4.9 Hz, 4H), 3.40 (q, J = 6.5 Hz, 2H), 2.48-2.58 (m, 6H); ^{13}C NMR (500 MHz, DMSO-*d*$_6$) δ 164.22, 159.07, 145.25, 144.98, 139.51, 138.40, 130.63, 126.84, 126.36, 125.13, 123.28, 120.96, 113.89, 111.96, 111.22, 109.10, 109.07, 103.13, 57.79, 52.95, 44.84, 36.66; HRMS (FAB) calc. for $C_{22}H_{21}F_3N_6O$, $[M+H]^+$: 443.1807, found: 443.1804.

N-(2-(4-(3-Chloropyridin-2-yl)piperazin-1-yl)ethyl)-5-cyano-1H-indole-3-carboxamide (27)

Yield 90%, white solid, mp: 243.3 °C; ^{1}H NMR (500 MHz, DMSO-*d*$_6$) δ 12.02 (s, 1H), 8.51 (d, J = 1.6 Hz, 1H), 8.15-8.20 (m, 2H), 8.01 (s, 1H), 7.75 (dd, J = 7.5, 1.6 Hz, 1H), 7.58 (dd, J = 8.5, 0.6 Hz, 1H), 7.47 (dd, J = 8.5, 1.9 Hz, 1H), 6.95 (dd, J = 7.8, 4.7 Hz, 1H), 3.39-3.45 (m, 2H), 3.24 (s, 4H), 2.62 (d, J = 36.4 Hz, 4H), 2.48-2.52 (m, 2H); ^{13}C NMR (500 MHz, DMSO-*d*$_6$) δ 164.23, 158.27, 146.55, 139.59, 138.40, 130.63, 126.84, 126.37, 125.13, 122.05, 120.96, 118.88, 113.91, 111.88, 103.13, 57.87, 53.22, 49.27, 36.65; HRMS (FAB) calc. for $C_{21}H_{21}ClN_6O$, $[M+H]^+$: 409.1544, found: 409.1548.

5-Cyano-N-(2-(4-(3-(trifluoromethyl)pyridin-2-yl)piperazin-1-yl)ethyl)-1H-indole-3-carboxamide (28)

Yield 49%, white solid, mp: 222.9 °C; ^{1}H NMR (500 MHz, DMSO-*d*$_6$) δ 12.02 (s, 1H), 8.50 (d, J = 0.9 Hz, 1H), 8.46 (dd, J = 4.7, 1.3 Hz, 1H), 8.15-8.17 (m, 1H), 7.99-8.02 (m, 2H), 7.57-7.60 (m, 1H), 7.47 (dd, J = 8.5, 1.6 Hz, 1H), 7.12 (ddd, J = 7.7, 4.9, 0.8 Hz, 1H), 3.39 (q, J = 6.6 Hz, 2H), 3.18 (t, J = 4.7 Hz, 4H), 2.55-2.65 (m, 4H), 2.50 (q, J = 7.1 Hz, 2H); ^{13}C NMR (500 MHz, DMSO-*d*$_6$) δ 164.24, 159.57, 152.09, 138.40, 138.23, 138.20, 130.61, 126.83, 126.36, 125.14, 120.96, 117.96, 115.79, 115.54, 113.91, 111.93, 103.13, 57.81, 53.32, 50.95, 36.66; HRMS (FAB) calc. for $C_{22}H_{21}F_3N_6O$, $[M+H]^+$: 443.1807, found: 443.1814.

5-Cyano-N-(2-(4-(quinolin-2-yl)piperazin-1-yl)ethyl)-1H-indole-3-carboxamide (29)

Yield 72%, white solid, mp: 228.2 °C; ^{1}H NMR (500 MHz, DMSO-*d*$_6$) δ 12.02 (s, 1H), 8.52-8.55 (m, 1H), 8.17 (d, J = 14.4 Hz, 1H), 8.03 (t, J = 5.7 Hz, 1H), 7.99 (d, J = 9.1 Hz, 1H), 7.64-7.69 (m, 1H), 7.57-7.62 (m, 1H), 7.52 (d, J = 7.8 Hz, 1H), 7.37-7.49 (m, 2H), 7.16-7.24 (m, 2H), 3.66 (t, J = 4.9 Hz, 4H), 3.38-3.47 (m, 2H), 2.48-2.60 (m, 6H); ^{13}C NMR (500 MHz, DMSO-*d*$_6$) δ 164.22, 157.61, 147.78, 138.41, 137.84,

 doi:10.20944/preprints202412.2383.v1

130.64, 129.88, 127.89, 126.85, 126.55, 126.37, 125.13, 123.26, 122.53, 120.97, 113.91, 111.97, 110.63, 103.13, 57.88, 53.31, 45.15, 36.70; HRMS (FAB) calc. for $C_{25}H_{24}N_6O$, $[M+H]^+$: 425.2090, found: 425.2102.

N-(2-(4-(2-Carbamoylbenzofuran-5-yl)piperazin-1-yl)ethyl)-5-cyano-1H-indole-3-carboxamide (30)

Yield 60%, white solid, mp: 258.4 °C; ^{1}H NMR (500 MHz, DMSO-d_6) δ 12.01 (s, 1H), 8.51 (t, J = 0.8 Hz, 1H), 8.15 (s, 1H), 7.97-8.02 (m, 2H), 7.58 (td, J = 4.2, 0.7 Hz, 1H), 7.53 (t, J = 9.1 Hz, 1H), 7.47 (dd, J = 8.5, 1.6 Hz, 1H), 7.43 (dd, J = 9.7, 0.9 Hz, 1H), 7.35-7.36 (m, 1H), 7.12-7.15 (m, 2H), 3.37-3.47 (m, 2H), 3.07-3.16 (m, 4H), 2.59-2.64 (m, 4H), 2.52 (t, J = 6.9 Hz, 2H); ^{13}C NMR (500 MHz, DMSO-d_6) δ 164.19, 160.42, 150.20, 149.62, 148.86, 138.40, 130.63, 128.26, 126.83, 126.35, 125.14, 120.97, 118.60, 113.92, 112.32, 111.97, 110.19, 108.07, 103.13, 57.82, 53.47, 50.34, 36.71; HRMS (FAB) calc. for $C_{25}H_{24}N_6O_3$, $[M+H]^+$: 457.1988, found: 457.1974.

5-Cyano-N-(2-(4-(2-((2,4-dimethylphenyl)thio)phenyl)piperazin-1-yl)ethyl)-1H-indole-3-carboxamide (31)

Yield 65%, white solid, mp: 247.2 °C; ^{1}H NMR (500 MHz, DMSO-d_6) δ 12.02 (d, J = 1.9 Hz, 1H), 8.52 (d, J = 1.6 Hz, 1H), 8.16 (d, J = 2.8 Hz, 1H), 8.01 (t, J = 5.5 Hz, 1H), 7.57-7.61 (m, 1H), 7.48 (dd, J = 8.5, 1.6 Hz, 1H), 7.29 (d, J = 7.8 Hz, 1H), 7.20 (d, J = 12.2 Hz, 1H), 7.10 (dd, J = 8.0, 1.4 Hz, 1H), 7.04-7.07 (m, 2H), 6.84-6.87 (m, 1H), 6.34 (dd, J = 7.8, 1.3 Hz, 1H), 3.39-3.47 (m, 2H), 2.98 (s, 4H), 2.60 (s, 4H), 2.54 (t, J = 6.6 Hz, 2H), 2.28-2.32 (m, 3H), 2.16-2.23 (m, 3H); ^{13}C NMR (500 MHz, DMSO-d_6) δ 164.20, 149.64, 142.19, 139.60, 138.41, 136.28, 133.87, 132.20, 130.65, 128.52, 127.93, 126.83, 126.34, 126.14, 125.14, 124.75, 120.99, 120.59, 113.92, 112.00, 103.13, 57.85, 53.72, 51.78, 36.72, 21.24, 20.63; HRMS (FAB) calc. for $C_{30}H_{31}N_5OS$, $[M+H]^+$: 510.2328, found: 510.2317.

N-(2-(4-(Benzo[d]isothiazol-3-yl)piperazin-1-yl)ethyl)-5-cyano-1H-indole-3-carboxamide (32)

Yield 52%, white solid, mp: 256.7 °C; ^{1}H NMR (500 MHz, DMSO-d_6) δ 12.03 (d, J = 1.9 Hz, 1H), 8.52-8.55 (m, 1H), 8.18 (dd, J = 14.8, 2.8 Hz, 1H), 8.04 (t, J = 5.5 Hz, 1H), 8.00-8.02 (m, 2H), 7.56-7.62 (m, 1H), 7.50-7.54 (m, 1H), 7.44-7.48 (m, 1H), 7.38-7.42 (m, 1H), 3.42 (t, J = 6.4 Hz, 6H), 2.74 (d, J = 63.4 Hz, 4H), 2.48-2.58 (m, 2H); ^{13}C NMR (500 MHz, DMSO-d_6) δ 164.27, 164.04, 152.52, 138.41, 130.65, 128.39, 127.88, 126.84, 126.37, 125.15, 124.93, 124.69, 121.58, 120.99, 113.92, 111.92, 103.14, 57.84, 53.11, 50.15, 36.64; HRMS (FAB) calc. for $C_{23}H_{22}N_6OS$, $[M+H]^+$: 431.1654, found: 431.1664.

5-Cyano-N-(2-(4-(4-fluorobenzoyl)piperazin-1-yl)ethyl)-1H-indole-3-carboxamide (33)

Yield 31%, white solid, mp: 148.1 °C; ^{1}H NMR (500 MHz, DMSO-d_6) δ 12.03 (s, 1H), 8.50 (d, J = 0.9 Hz, 1H), 8.14 (d, J = 2.3 Hz, 1H), 8.01 (t, J = 5.5 Hz, 1H), 7.57-7.66 (m, 1H), 7.47 (dd, J = 8.3, 1.4 Hz, 1H), 7.38-7.44 (m, 2H), 7.21-7.25 (m, 2H), 3.49-3.76 (m, 2H), 3.34-3.46 (m, 4H), 2.48-2.63 (m, 4H), 2.44-2.32 (2H); ^{13}C NMR (500 MHz, DMSO-d_6) δ 168.54, 164.19, 164.00, 162.05, 138.40, 132.88, 132.85, 130.62, 130.07, 129.99, 126.83, 126.34, 125.13, 120.97, 115.99, 115.81, 113.91, 111.95, 103.12, 57.58, 53.15, 42.29, 36.59; HRMS (FAB) calc. for $C_{23}H_{22}FN_5O_2$, $[M+H]^+$: 420.1836, found: 420.1844.

5-Cyano-N-(2-(4-(3-(trifluoromethyl)benzoyl)piperazin-1-yl)ethyl)-1H-indole-3-carboxamide (34)

Yield 71%, white solid, mp: 143.5 °C; ^{1}H NMR (500 MHz, DMSO-d_6) δ 12.12 (d, J = 68.4 Hz, 1H), 8.51-8.68 (m, 1H), 8.15-8.19 (m, 1H), 7.97-8.09 (m, 1H), 7.54-7.69 (m, 1H), 7.46-7.53 (m, 1H), 7.24-7.42 (m, 1H), 7.18 (d, J = 8.5 Hz, 1H), 7.13 (d, J = 12.9 Hz, 1H), 7.01-7.05 (m, 1H), 3.38-3.47 (m, 2H), 3.20 (t, J = 4.9 Hz, 4H), 2.56-2.63 (m, 4H), 2.51 (t, J = 7.1 Hz, 2H); ^{13}C NMR (500 MHz, DMSO-d_6) δ 164.20, 151.77, 138.41, 130.64, 130.50, 130.46, 130.26, 126.83, 126.36, 126.07, 125.12, 123.91, 120.97, 119.18, 115.00, 113.91, 111.95, 111.31, 103.12, 57.75, 53.13, 48.14, 36.67; HRMS (FAB) calc. for $C_{24}H_{22}F_3N_5O_2$, $[M+H]^+$: 470.1804, found: 470.1817.

5-Cyano-N-(2-(4-(2,3-dihydrobenzo[b][1,4]dioxine-2-carbonyl)piperazin-1-yl)ethyl)-1H-indole-3-carboxamide (35)

Yield 83%, white solid, mp: 140.2 °C; ^{1}H NMR (500 MHz, DMSO-d_6) δ 12.02 (s, 1H), 8.51 (s, 1H), 8.15 (s, 1H), 7.96-8.01 (m, 1H), 7.58 (d, J = 8.5 Hz, 1H), 7.48 (dd, J = 8.5, 1.3 Hz, 1H), 6.84-6.86 (m, 1H), 6.78-6.83 (m, 3H), 5.17 (dd, J = 6.4, 2.4 Hz, 1H), 4.33 (dd, J = 11.9, 2.5 Hz, 1H), 4.13 (dd, J = 11.8, 6.4 Hz, 1H), 3.36-3.59 (m, 6H), 2.48-2.60 (m, 4H), 2.35 (d, J = 27.6 Hz, 2H); ^{13}C NMR (500 MHz, DMSO-d_6) δ 165.17, 164.20, 143.58, 143.39, 138.40, 130.63, 126.84, 126.35, 125.14, 121.97, 121.85, 120.97, 117.52,

 doi:10.20944/preprints202412.2383.v1

117.38, 113.91, 111.95, 103.13, 69.91, 65.25, 57.58, 53.50, 52.95, 45.60, 42.00, 36.57; HRMS (FAB) calc. for $C_{25}H_{25}N_5O_4$, $[M+H]^+$: 460.1985, found: 460.1987.

5-Cyano-N-(3-(4-(3-fluorophenyl)piperazin-1-yl)propyl)-1H-indole-3-carboxamide (36)

Yield 33%, white solid, mp: 229.9 °C; ^{1}H NMR (500 MHz, DMSO-*d*$_6$) δ 12.02 (s, 1H), 8.50 (t, J = 0.8 Hz, 1H), 8.14-8.17 (m, 1H), 7.96-8.06 (m, 1H), 7.57 (dd, J = 8.5, 0.6 Hz, 1H), 7.46 (dd, J = 8.5, 1.9 Hz, 1H), 7.16 (q, J = 8.0 Hz, 1H), 6.66-6.71 (m, 2H), 6.48 (td, J = 8.2, 2.3 Hz, 1H), 3.28 (q, J = 6.5 Hz, 2H), 3.12 (t, J = 5.0 Hz, 4H), 2.46 (q, J = 1.9 Hz, 4H), 2.32-2.38 (m, 2H), 1.66-1.75 (m, 3H); ^{13}C NMR (500 MHz, DMSO-*d*$_6$) δ 164.84, 164.24, 162.86, 153.34, 138.40, 130.83, 130.75, 130.54, 126.88, 126.44, 125.07, 121.00, 113.89, 111.97, 111.30, 111.28, 105.14, 104.98, 103.04, 102.26, 102.06, 56.16, 53.13, 48.21, 37.58, 27.22; HRMS (FAB) calc. for $C_{23}H_{24}FN_5O$, $[M+H]^+$: 406.2043, found: 406.2031.

N-(3-(4-(3-Chlorophenyl)piperazin-1-yl)propyl)-5-cyano-1H-indole-3-carboxamide (37)

Yield 61%, white solid, mp: 240.1 °C; ^{1}H NMR (500 MHz, DMSO-*d*$_6$) δ 12.00 (s, 1H), 8.51-8.54 (m, 1H), 8.15 (d, J = 2.5 Hz, 1H), 7.96-8.06 (m, 1H), 7.56-7.59 (m, 1H), 7.46-7.50 (m, 1H), 7.14-7.18 (m, 1H), 6.88 (t, J = 2.2 Hz, 1H), 6.83-6.85 (m, 1H), 6.72-6.74 (m, 1H), 3.27 (t, J = 6.7 Hz, 2H), 3.11-3.13 (m, 4H), 2.46 (q, J = 1.9 Hz, 4H), 2.27-2.38 (m, 2H), 1.66-1.75 (m, 2H); ^{13}C NMR (500 MHz, DMSO-*d*$_6$) δ 164.23, 152.79, 138.39, 134.32, 130.91, 130.47, 126.90, 126.43, 125.11, 120.99, 118.46, 114.96, 114.09, 113.86, 111.99, 103.08, 56.15, 53.12, 48.18, 37.57, 27.21; HRMS (FAB) calc. for $C_{23}H_{24}ClN_5O$, $[M+H]^+$: 422.1748, found: 422.1739.

5-Cyano-N-(3-(4-(3-(trifluoromethyl)phenyl)piperazin-1-yl)propyl)-1H-indole-3-carboxamide (38)

Yield 27%, white solid, mp: 208.1 °C; ^{1}H NMR (500 MHz, DMSO-*d*$_6$) δ 12.00 (s, 1H), 8.51 (q, J = 0.7 Hz, 1H), 8.14 (d, J = 3.5 Hz, 1H), 8.05 (t, J = 5.5 Hz, 1H), 7.57 (dd, J = 8.5, 0.6 Hz, 1H), 7.47 (dd, J = 8.5, 1.6 Hz, 1H), 7.37 (t, J = 8.0 Hz, 1H), 7.17 (dd, J = 8.5, 2.5 Hz, 1H), 7.11 (s, 1H), 7.01 (d, J = 7.5 Hz, 1H), 3.27 (d, J = 7.2 Hz, 2H), 3.13-3.21 (m, 4H), 2.49 (t, J = 5.0 Hz, 4H), 2.37 (t, J = 7.1 Hz, 2H), 1.67-1.75 (m, 2H); ^{13}C NMR (500 MHz, DMSO-*d*$_6$) δ 164.23, 151.77, 138.39, 130.47, 130.26, 126.89, 126.42, 126.05, 125.11, 123.88, 120.99, 119.16, 115.02, 113.87, 111.99, 111.22, 103.07, 56.16, 53.12, 48.14, 37.58, 27.22; HRMS (FAB) calc. for $C_{24}H_{24}F_3N_5O$, $[M+H]^+$: 456.2011, found: 456.2025.

5-Cyano-N-(3-(4-(4-fluorophenyl)piperazin-1-yl)propyl)-1H-indole-3-carboxamide (39)

Yield 34%, white solid, mp: 240.2 °C; ^{1}H NMR (500 MHz, DMSO-*d*$_6$) δ 12.14 (s, 1H), 8.51 (d, J = 1.6 Hz, 1H), 8.34 (s, 1H), 8.24 (d, J = 2.5 Hz, 1H), 7.59 (d, J = 8.5 Hz, 1H), 7.48 (dd, J = 8.5, 1.6 Hz, 1H), 7.03-7.15 (m, 2H), 6.97 (q, J = 4.5 Hz, 2H), 3.41-3.67 (m, 4H), 3.33 (t, J = 6.3 Hz, 2H), 3.05-3.11 (m, 6H), 1.90-2.04 (m, 2H); ^{13}C NMR (500 MHz, DMSO-*d*$_6$) δ 164.73, 138.42, 130.87, 126.82, 126.36, 125.17, 120.99, 118.35, 118.26, 116.09, 115.91, 113.95, 111.66, 103.15, 53.91, 42.20, 18.54, 17.25, 12.72; HRMS (FAB) calc. for $C_{23}H_{24}FN_5O$, $[M+H]^+$: 406.2043, found: 406.2039.

N-(3-(4-(4-Chlorophenyl)piperazin-1-yl)propyl)-5-cyano-1H-indole-3-carboxamide (40)

Yield 19%, white solid, mp: 241.8 °C; ^{1}H NMR (500 MHz, DMSO-*d*$_6$) δ 12.00 (s, 1H), 8.50 (q, J = 0.8 Hz, 1H), 8.14 (s, 1H), 8.05 (t, J = 5.7 Hz, 1H), 7.57 (dd, J = 8.5, 0.6 Hz, 1H), 7.47 (dd, J = 8.5, 1.6 Hz, 1H), 7.16-7.19 (m, 2H), 6.89 (td, J = 6.4, 3.8 Hz, 2H), 3.24-3.28 (m, 2H), 3.07-3.12 (m, 4H), 2.47-2.48 (m, 4H), 2.32-2.37 (m, 2H), 1.66-1.74 (m, 2H); ^{13}C NMR (500 MHz, DMSO-*d*$_6$) δ 164.23, 150.38, 138.39, 130.47, 129.10, 126.89, 126.42, 125.11, 122.73, 120.99, 117.27, 113.87, 111.99, 103.07, 56.16, 53.15, 48.56, 37.58, 27.21; HRMS (FAB) calc. for $C_{23}H_{24}ClN_5O$, $[M+H]^+$: 422.1748, found: 422.1745.

5-Cyano-N-(3-(4-(4-(trifluoromethyl)phenyl)piperazin-1-yl)propyl)-1H-indole-3-carboxamide (41)

Yield 38%, white solid, mp: 250.7 °C; ^{1}H NMR (500 MHz, DMSO-*d*$_6$) δ 12.00 (s, 1H), 8.51 (d, J = 0.9 Hz, 1H), 8.15 (d, J = 2.5 Hz, 1H), 8.05 (t, J = 5.7 Hz, 1H), 7.57 (dd, J = 8.5, 0.9 Hz, 1H), 7.44-7.48 (m, 3H), 7.01 (d, J = 8.8 Hz, 2H), 3.26 (s, 2H), 3.23 (t, J = 5.0 Hz, 4H), 2.48 (t, J = 4.7 Hz, 4H), 2.32-2.38 (m, 2H), 1.67-1.75 (m, 2H); ^{13}C NMR (500 MHz, DMSO-*d*$_6$) δ 164.23, 153.81, 138.39, 130.47, 126.89, 126.68, 126.64, 126.42, 125.11, 120.99, 118.43, 118.14, 114.62, 113.87, 111.99, 103.08, 56.14, 53.01, 47.53, 37.55, 27.21; HRMS (FAB) calc. for $C_{24}H_{24}F_3N_5O$, $[M+H]^+$: 456.2011, found: 456.2025.

5-Cyano-N-(3-(4-(6-(trifluoromethyl)pyridin-2-yl)piperazin-1-yl)propyl)-1H-indole-3-carboxamide (42)

 doi:10.20944/preprints202412.2383.v1

Yield 82%, white solid, mp: 230.7 °C; ^{1}H NMR (500 MHz, DMSO-*d*$_6$) δ 12.02 (s, 1H), 8.51-8.54 (m, 1H), 8.15-8.19 (m, 1H), 8.02-8.07 (m, 1H), 7.67-7.76 (m, 1H), 7.53-7.61 (m, 1H), 7.43-7.51 (m, 1H), 7.06-7.11 (m, 1H), 6.98 (d, J = 7.2 Hz, 1H), 3.58 (d, J = 69.1 Hz, 4H), 3.27 (d, J = 7.2 Hz, 2H), 2.44 (s, 4H), 2.32-2.38 (m, 2H), 1.62-1.73 (m, 2H); ^{13}C NMR (500 MHz, DMSO-*d*$_6$) δ 164.24, 159.07, 144.94, 139.52, 138.39, 130.48, 126.90, 126.44, 125.09, 123.28, 120.99, 113.86, 111.97, 111.22, 109.29, 103.07, 56.18, 52.95, 44.81, 37.54, 27.03; HRMS (FAB) calc. for $C_{23}H_{23}F_3N_6O$, $[M+H]^+$: 457.1964, found: 457.1977.

N-(3-(4-(3-Chloropyridin-2-yl)piperazin-1-yl)propyl)-5-cyano-1H-indole-3-carboxamide (43)

Yield 93%, white solid, mp: 201.8 °C; ^{1}H NMR (500 MHz, DMSO-*d*$_6$) δ 12.02 (s, 1H), 8.51-8.54 (m, 1H), 8.15-8.21 (m, 2H), 7.99-8.08 (m, 1H), 7.73-7.77 (m, 1H), 7.53-7.61 (m, 1H), 7.42-7.49 (m, 1H), 6.93-6.98 (m, 1H), 3.23-3.27 (m, 6H), 2.51-2.77 (m, 4H), 2.32-2.40 (m, 2H), 1.58-1.73 (m, 2H); ^{13}C NMR (500 MHz, DMSO-*d*$_6$) δ 164.25, 158.23, 146.55, 139.58, 138.39, 130.48, 126.90, 126.44, 125.09, 122.05, 120.99, 118.95, 113.86, 111.98, 103.07, 56.19, 53.15, 49.20, 37.53, 26.99; HRMS (FAB) calc. for $C_{22}H_{23}ClN_6O$, $[M+H]^+$: 423.1700, found: 423.1696.

5-Cyano-N-(3-(4-(3-(trifluoromethyl)pyridin-2-yl)piperazin-1-yl)propyl)-1H-indole-3-carboxamide (44)

Yield 63%, white solid, mp: 201.9 °C; ^{1}H NMR (500 MHz, DMSO-*d*$_6$) δ 12.01 (s, 1H), 8.50-8.53 (m, 1H), 8.47 (dd, J = 4.7, 1.6 Hz, 1H), 8.15-8.18 (m, 1H), 8.05-8.10 (m, 1H), 7.96-8.01 (m, 1H), 7.57-7.61 (m, 1H), 7.47 (dd, J = 8.5, 1.6 Hz, 1H), 7.13 (dd, J = 7.7, 4.9 Hz, 1H), 3.27 (t, J = 6.4 Hz, 2H), 3.17 (t, J = 4.6 Hz, 4H), 2.51-2.65 (m, 4H), 2.32-2.41 (m, 2H), 1.67-1.75 (m, 2H); ^{13}C NMR (500 MHz, DMSO-*d*$_6$) δ 164.27, 159.55, 152.10, 138.39, 138.23, 138.19, 130.48, 126.89, 126.42, 125.58, 125.11, 123.38, 120.99, 118.04, 115.72, 113.87, 111.96, 103.08, 56.09, 53.22, 50.86, 37.50, 27.07; HRMS (FAB) calc. for $C_{23}H_{23}F_3N_6O$, $[M+H]^+$: 457.1964, found: 457.1977.

5-Cyano-N-(3-(4-(quinolin-2-yl)piperazin-1-yl)propyl)-1H-indole-3-carboxamide (45)

Yield 44%, white solid, mp: 215.2 °C; ^{1}H NMR (500 MHz, DMSO-*d*$_6$) δ 12.07 (s, 1H), 8.52 (s, 1H), 8.17 (s, 1H), 8.13 (s, 1H), 8.00 (d, J = 9.2 Hz, 1H), 7.66 (d, J = 7.8 Hz, 1H), 7.58 (d, J = 8.3 Hz, 1H), 7.38-7.54 (m, 3H), 7.16-7.28 (m, 2H), 3.80 (d, J = 114.0 Hz, 4H), 3.46-3.34 (2H), 2.71 (d, J = 133.7 Hz, 4H), 2.03-2.29 (m, 2H), 1.74 (s, 2H); ^{13}C NMR (500 MHz, DMSO-*d*$_6$) δ 172.54, 164.32, 147.72, 138.41, 137.92, 130.55, 129.93, 127.91, 126.89, 126.56, 126.43, 125.12, 123.32, 122.64, 121.00, 113.89, 111.92, 110.64, 103.10, 56.14, 53.27, 44.78, 37.31, 21.59; HRMS (FAB) calc. for $C_{26}H_{26}N_6O$, $[M+H]^+$: 439.2246, found: 439.2248.

N-(3-(4-(2-Carbamoylbenzofuran-5-yl)piperazin-1-yl)propyl)-5-cyano-1H-indole-3-carboxamide (46)

Yield 81%, white solid, mp: 243.5 °C; ^{1}H NMR (500 MHz, DMSO-*d*$_6$) δ 12.02 (s, 1H), 8.51 (d, J = 1.3 Hz, 1H), 8.15 (d, J = 2.8 Hz, 1H), 8.07 (t, J = 5.7 Hz, 1H), 7.97 (s, 1H), 7.55-7.58 (m, 2H), 7.47 (dd, J = 8.5, 1.6 Hz, 1H), 7.43 (dd, J = 9.4, 0.9 Hz, 1H), 7.36 (d, J = 0.9 Hz, 1H), 7.12-7.14 (m, 2H), 3.09 (t, J = 4.4 Hz, 4H), 2.53-2.60 (m, 4H), 2.32-2.41 (m, 2H), 1.87-2.04 (m, 2H), 1.72 (td, J = 14.0, 6.8 Hz, 2H); ^{13}C NMR (500 MHz, DMSO-*d*$_6$) δ 164.24, 160.29, 150.07, 149.58, 148.83, 138.26, 130.48, 128.26, 126.90, 125.11, 121.00, 118.59, 113.87, 112.32, 111.99, 110.20, 108.05, 103.07, 56.18, 53.43, 50.29, 40.65, 40.56, 40.48, 40.39, 40.32, 40.23, 40.15, 40.06, 39.98, 39.89, 39.73, 39.56, 37.60, 27.21; HRMS (FAB) calc. for $C_{26}H_{26}N_6O_3$, $[M+H]^+$: 471.2145, found: 471.2144.

5-Cyano-N-(3-(4-(2-((2,4-dimethylphenyl)thio)phenyl)piperazin-1-yl)propyl)-1H-indole-3-carboxamide (47)

Yield 22%, white solid, mp: 217.7 °C; ^{1}H NMR (500 MHz, DMSO-*d*$_6$) δ 12.02 (d, J = 1.6 Hz, 1H), 8.51-8.54 (m, 1H), 8.16-8.19 (m, 1H), 8.08 (t, J = 5.7 Hz, 1H), 7.58 (d, J = 8.5 Hz, 1H), 7.47 (dd, J = 8.5, 1.6 Hz, 1H), 7.27-7.31 (m, 1H), 7.19 (d, J = 15.1 Hz, 1H), 7.03-7.08 (m, 3H), 6.83-6.89 (m, 1H), 6.33-6.35 (m, 1H), 3.28 (t, J = 6.6 Hz, 2H), 2.95-3.09 (m, 4H), 2.48-2.65 (m, 4H), 2.42 (s, 2H), 2.24-2.31 (m, 3H), 2.16-2.22 (m, 3H), 1.68-1.76 (m, 2H); ^{13}C NMR (500 MHz, DMSO-*d*$_6$) δ 164.27, 149.59, 142.18, 139.60, 138.40, 136.27, 133.87, 132.19, 130.50, 128.51, 127.91, 126.90, 126.42, 126.33, 126.14, 125.12, 124.76, 121.00, 120.54, 113.87, 112.00, 103.08, 56.21, 53.63, 51.70, 37.60, 27.11, 21.23, 20.62; HRMS (FAB) calc. for $C_{31}H_{33}N_5OS$, $[M+H]^+$: 524.2484, found: 524.2486.

 doi:10.20944/preprints202412.2383.v1

N-(3-(4-(Benzo[d]isothiazol-3-yl)piperazin-1-yl)propyl)-5-cyano-1H-indole-3-carboxamide (48)

Yield 43%, white solid, mp: 227.0 °C; ^{1}H NMR (500 MHz, DMSO-*d*$_6$) δ 12.03 (d, J = 1.9 Hz, 1H), 8.35-8.51 (m, 1H), 8.17 (dd, J = 11.8, 3.3 Hz, 1H), 8.05-8.10 (m, 1H), 8.01 (d, J = 9.1 Hz, 2H), 7.57-7.65 (m, 1H), 7.50-7.53 (m, 1H), 7.44-7.49 (m, 1H), 7.37-7.41 (m, 1H), 3.43 (s, 4H), 3.29 (t, J = 6.6 Hz, 2H), 2.60-2.76 (m, 4H), 2.47 (d, J = 1.9 Hz, 2H), 1.70-1.76 (m, 2H); ^{13}C NMR (500 MHz, DMSO-*d*$_6$) δ 164.29, 163.98, 152.52, 138.40, 130.50, 128.40, 127.86, 126.89, 126.42, 125.13, 124.94, 124.67, 121.59, 121.00, 113.88, 111.96, 103.08, 56.14, 55.42, 53.01, 50.02, 37.49, 27.07; HRMS (FAB) calc. for $C_{24}H_{24}N_6OS$, $[M+H]^+$: 445.1811, found: 445.1814.

5-Cyano-N-(3-(4-(4-fluorobenzoyl)piperazin-1-yl)propyl)-1H-indole-3-carboxamide (49)

Yield 29%, white solid, mp: 140.3 °C; ^{1}H NMR (500 MHz, DMSO-*d*$_6$) δ 12.02 (s, 1H), 8.50 (s, 1H), 8.14 (d, J = 1.8 Hz, 1H), 8.06 (t, J = 5.3 Hz, 1H), 7.57 (d, J = 8.3 Hz, 1H), 7.47 (dd, J = 8.5, 1.6 Hz, 1H), 7.41 (ddd, J = 11.9, 5.3, 3.2 Hz, 2H), 7.20-7.26 (m, 2H), 3.51 (d, J = 40.0 Hz, 2H), 3.25 (q, J = 6.4 Hz, 4H), 2.34 (t, J = 7.1 Hz, 6H), 1.62-1.74 (m, 2H); ^{13}C NMR (500 MHz, DMSO-*d*$_6$) δ 168.51, 164.23, 162.00, 138.39, 132.88, 130.48, 130.06, 129.99, 126.88, 126.42, 125.11, 120.99, 115.99, 115.81, 113.87, 111.96, 103.07, 55.98, 53.10, 47.89, 37.47, 27.17; HRMS (FAB) calc. for $C_{24}H_{24}FN_5O_2$, $[M+H]^+$: 434.1992, found: 434.1988.

5-Cyano-N-(3-(4-(3-(trifluoromethyl)benzoyl)piperazin-1-yl)propyl)-1H-indole-3-carboxamide (50)

Yield 36%, white solid, mp: 142.8 °C; ^{1}H NMR (500 MHz, DMSO-*d*$_6$) δ 12.01 (s, 1H), 8.51-8.54 (m, 1H), 8.15-8.18 (m, 1H), 8.05 (t, J = 5.5 Hz, 1H), 7.56-7.61 (m, 1H), 7.46-7.50 (m, 1H), 7.35-7.41 (m, 1H), 7.16-7.22 (m, 1H), 7.11 (s, 1H), 7.00-7.05 (m, 1H), 3.28-3.38 (m, 2H), 3.14-3.18 (m, 4H), 2.48 (t, J = 4.6 Hz, 4H), 2.32-2.39 (m, 2H), 1.67-1.73 (m, 2H); ^{13}C NMR (500 MHz, DMSO-*d*$_6$) δ 164.23, 151.76, 138.39, 130.48, 130.46, 130.26, 126.90, 126.43, 126.07, 125.09, 123.90, 120.99, 119.15, 114.99, 113.86, 111.99, 111.29, 111.26, 103.08, 56.16, 53.12, 48.14, 37.58, 27.23; HRMS (FAB) calc. for $C_{25}H_{24}F_3N_5O_2$, $[M+H]^+$: 484.1960, found: 484.1956.

5-Cyano-N-(3-(4-(2,3-dihydrobenzo[b][1,4]dioxine-2-carbonyl)piperazin-1-yl)propyl)-1H-indole-3-carboxamide (51)

Yield 82%, white solid, mp: 143.1 °C; ^{1}H NMR (500 MHz, DMSO-*d*$_6$) δ 11.94 (d, J = 65.6 Hz, 1H), 8.48-8.51 (m, 1H), 8.16 (d, J = 15.1 Hz, 1H), 8.00-8.06 (m, 1H), 7.52-7.62 (m, 1H), 7.42-7.52 (m, 1H), 6.83-6.90 (m, 1H), 6.68-6.82 (m, 3H), 5.13-5.26 (m, 1H), 4.27-4.34 (m, 1H), 4.13 (dd, J = 11.6, 6.6 Hz, 1H), 3.38-3.57 (m, 4H), 3.27 (q, J = 6.6 Hz, 2H), 2.29-2.43 (m, 6H), 1.65-1.70 (m, 2H); ^{13}C NMR (500 MHz, DMSO-*d*$_6$) δ 165.15, 164.24, 143.56, 143.37, 138.39, 130.48, 126.89, 126.42, 125.12, 121.98, 121.87, 120.99, 117.53, 117.38, 113.87, 111.97, 103.08, 69.91, 65.24, 55.97, 53.54, 52.95, 45.59, 41.99, 37.48, 27.16; HRMS (FAB) calc. for $C_{26}H_{27}N_5O_4$, $[M+H]^+$: 474.2141, found: 474.2135.

5-Cyano-N-(2-(4-(6-fluorobenzo[d]isoxazol-3-yl)piperidin-1-yl)ethyl)-1H-indole-3-carboxamide (52)

Yield 88%, white solid, mp: 208.9 °C; ^{1}H NMR (500 MHz, DMSO-*d*$_6$) δ 12.02 (s, 1H), 8.51 (d, J = 1.6 Hz, 1H), 8.16 (d, J = 2.8 Hz, 1H), 7.95-8.00 (m, 2H), 7.64 (dd, J = 9.1, 1.9 Hz, 1H), 7.58 (dd, J = 8.5, 0.6 Hz, 1H), 7.48 (dd, J = 8.5, 1.6 Hz, 1H), 7.22 (td, J = 9.1, 2.2 Hz, 1H), 3.39-3.47 (m, 2H), 3.12 (s, 1H), 3.01 (d, J = 8.2 Hz, 2H), 2.48-2.58 (m, 2H), 2.18 (s, 2H), 1.99-2.04 (m, 2H), 1.84 (t, J = 10.8 Hz, 2H); ^{13}C NMR (500 MHz, DMSO-*d*$_6$) δ 165.18, 164.26, 163.59, 163.15, 138.44, 130.62, 126.84, 126.35, 125.14, 124.37, 124.28, 120.96, 117.77, 113.91, 113.13, 112.89, 111.87, 103.13, 97.97, 97.71, 57.89, 53.55, 37.05, 33.80, 30.58; HRMS (FAB) calc. for $C_{23}H_{21}FN_6O_2$, $[M+H]^+$: 432.1836, found: 432.1834.

N-(2-(4-(5-Chloro-2-oxo-2,3-dihydro-1H-benzo[d]imidazol-1-yl)piperidin-1-yl)ethyl)-5-cyano-1H-indole-3-carboxamide (53)

Yield 90%, white solid, mp: 266.7 °C; ^{1}H NMR (500 MHz, DMSO-*d*$_6$) δ 12.06 (s, 1H), 10.99 (s, 1H), 8.51 (d, J = 0.9 Hz, 1H), 8.17 (d, J = 2.5 Hz, 1H), 8.03 (s, 1H), 7.59 (dd, J = 8.5, 0.9 Hz, 1H), 7.48 (dd, J = 8.5, 1.6 Hz, 1H), 7.15 (d, J = 8.5 Hz, 1H), 6.91-6.95 (m, 2H), 4.11 (s, 1H), 3.37-3.49 (m, 2H), 3.03-3.13 (m, 2H), 2.48-2.60 (m, 2H), 2.29 (q, J = 11.2 Hz, 2H), 2.13 (d, J = 7.5 Hz, 2H), 1.61-1.72 (m, 2H); ^{13}C NMR (500 MHz, DMSO-*d*$_6$) δ 164.28, 154.20, 138.42, 130.65, 129.94, 128.68, 126.85, 126.40, 125.27, 125.14,

 doi:10.20944/preprints202412.2383.v1

120.97, 120.52, 113.92, 111.93, 110.30, 109.21, 103.13, 57.59, 53.26, 50.82, 37.08, 29.06; HRMS (FAB) calc. for $C_{23}H_{22}ClN_7O_2$, $[M+H]^+$: 463.1649, found: 463.1659.

5-Cyano-N-(3-(4-(6-fluorobenzo[d]isoxazol-3-yl)piperidin-1-yl)propyl)-1H-indole-3-carboxamide (54)

Yield 96%, white solid, mp: 224.1 °C; ^{1}H NMR (500 MHz, DMSO-d_6) δ 12.02 (s, 1H), 8.51-8.54 (m, 1H), 8.16-8.19 (m, 1H), 8.07 (t, J = 5.3 Hz, 1H), 7.94-8.01 (m, 1H), 7.62-7.69 (m, 1H), 7.55-7.58 (m, 1H), 7.36-7.53 (m, 1H), 7.22 (td, J = 8.9, 2.1 Hz, 1H), 3.27 (d, J = 6.9 Hz, 2H), 3.11 (t, J = 11.1 Hz, 1H), 2.98 (s, 2H), 2.32-2.41 (m, 2H), 2.10 (s, 2H), 1.93-2.01 (m, 2H), 1.78-1.90 (m, 2H), 1.68-1.74 (m, 2H); ^{13}C NMR (500 MHz, DMSO-d_6) δ 165.14, 164.25, 163.58, 163.47, 163.17, 161.73, 138.40, 130.48, 126.89, 126.43, 125.09, 124.35, 124.25, 120.99, 117.77, 113.87, 113.10, 112.90, 111.99, 103.07, 97.96, 97.75, 56.27, 53.47, 37.55, 33.66, 30.41, 26.87; HRMS (FAB) calc. for $C_{24}H_{23}FN_6O_2$, $[M+H]^+$: 446.1992, found: 446.2002.

N-(3-(4-(5-Chloro-2-oxo-2,3-dihydro-1H-benzo[d]imidazol-1-yl)piperidin-1-yl)propyl)-5-cyano-1H-indole-3-carboxamide (55)

Yield 82%, white solid, mp: 197.8 °C; ^{1}H NMR (500 MHz, DMSO-d_6) δ 12.02 (s, 1H), 10.98 (s, 1H), 8.47-8.55 (m, 1H), 8.16 (d, J = 2.2 Hz, 1H), 8.03-8.08 (m, 1H), 7.57-7.62 (m, 1H), 7.47 (dd, J = 8.5, 1.6 Hz, 1H), 7.16 (d, J = 8.5 Hz, 1H), 6.96 (dd, J = 9.9, 1.7 Hz, 2H), 4.10 (t, J = 11.9 Hz, 1H), 3.27 (s, 2H), 2.93-3.01 (m, 2H), 2.40 (s, 2H), 2.25-2.32 (m, 2H), 1.84-2.04 (m, 2H), 1.68-1.75 (m, 2H), 1.61-1.63 (m, 2H); ^{13}C NMR (500 MHz, DMSO-d_6) δ 164.25, 154.20, 138.40, 130.49, 130.08, 128.70, 126.89, 126.43, 125.28, 125.11, 120.99, 120.57, 113.88, 111.99, 110.29, 109.21, 103.07, 55.92, 53.20, 50.97, 37.55, 29.15, 27.36; HRMS (FAB) calc. for $C_{24}H_{24}ClN_7O_2$, $[M+H]^+$: 477.1806, found: 477.1815.

3.2. In Vitro Receptor Assay

The screening of pain-related receptors for the mechanism of action study of compound **29** was conducted by outsourcing the experiment to Eurofins (https://www.eurofins.com).

3.3. In Vivo Assay

3.3.1. Animals

ICR male mice weighing 23–25 g were purchased from Samtako Korea (Osan, Korea). ICR mice were housed four per cage in a room with 12 h light–dark cycles. The temperature and relative humidity of the room were maintained at 22 ± 2 °C and 50 ± 5%, respectively. Food and water were available ad libitum. The procedures for animal testing were approved by Medifron Animal Care and Use Committees (Approval number; Medifron 2019-9). Efforts were made to minimize animal suffering and to reduce the number of animals used.

3.3.2. Formalin Model Test

Mice were randomly assigned to five groups (four per group) and single-dose drugs were administered by intraperitoneal injection. The formalin-induced licking paw test was modified from the method described by Dubuisson and Dennis [14]. Each mouse was acclimated to an acrylic observation chamber for at least 30 min before the injection of formalin. Twenty microliters of 2% formalin was injected subcutaneously into the right side of the hind paw. Each mouse was then placed in an individual clear plastic observational chamber (15×15×15), and the pain response was recorded for a period of 30 min. The summation of time (in seconds) spent in licking and biting responses of the injected paw during each 5 min block was measured as an indicator of the pain response. The first period (early phase) was recorded 0-5 min after the injection of formalin, and the second period (late phase) was recorded 20-30 min after the injection. The test compound was administered intraperitoneally 30 min before the formalin injection at three different doses: 0.1, 1, 5, and 10 mg/Kg. The vehicle was DMSO/Cremophor EL/D.W. (10/10/80). The data were expressed as the mean ± standard error of the mean (SEM). Statistical analysis was assessed by one-way analysis

 doi:10.20944/preprints202412.2383.v1

of variance (ANOVA) with Bonferroni's post-hoc test. Statistical significance was set at p-value < 0.05, with values of p <0.001 considered highlt significant.

3.3.3. Spinal Nerve Ligation (SNL) Model Test

Ligation of the left L5 and L6 spinal nerves in the rats was used as an experimental model of neuropathic pain. The rats were anesthetized by inhalation of 4% isoflurane in 95% of O_2, and anesthesia was maintained throughout the surgery. The surgical procedure was performed according to the method described by Kim and Chung [20]. The left L5 spinal nerve was isolated and ligated tightly with 6–0 black silk. The wound was closed in anatomical layers, with the skin being closed with stainless steel wound clips. The animals were then allowed to recover after the surgery. The behavioral signs representing neuropathic pain (mechanical allodynia) were examined in all the rats for 2 weeks postoperatively. The mechanical withdrawal threshold to the application of a von Frey filament (Stoelting, Wood Dale, IL, USA) was measured by using the up–down method [21]. The most sensitive area was first determined by poking various areas of the paw with a von Frey hair. Next, the actual test was conducted by gently poking various areas of the spot with the filament. A von Frey filament was applied 10 times (once every 3–4 sec) to each hind paw. The forces of the von Frey filaments ranged from 0.8 to 15 g. The frequency of foot withdrawal expressed as a percentage was used as the index of mechanical allodynia. The animals received the vehicle or drug by intraperitoneal injection. The vehicle was DMSO/Cremophor EL/D.W. (10/10/80). The test compound was administered at two different doses: 50 and 100 mg/Kg. The measurements to assess mechanical allodynia were taken at 1 , 3 and 5 hr after dosing. The results were analyzed using Student's t-test and are presented as the mean ± SEM. Statistical significance was set at $p < 0.05$.

3.3.4. Statistical Analysis

The results from the PC12 differentiation assay were reported as mean ± SEM of three different experiments and were evaluated using ANOVA followed by Dunnett's post hoc test. The results from the water permeability assay were expressed as means ± SEM of 4–15 single shots (time course curves) for each of the 4–6 different experiments and were analyzed by ANOVA, followed by the Newman–Keuls Q test. The results from the in vivo toxicity in the zebrafish model were reported as the mean of the values assessed using a sample score sheet, as reported by Brannen KC and colleagues. The formalin assay results are presented as the mean ± SEM for 8 mice per group and were analyzed using one-way analysis of variance (ANOVA) with Bonferroni's post hoc test. In addition, the data from Chung's neuropathic pain model are expressed as the mean ± SEM and were analyzed using Student's t-test. The data were considered to be statistically significant if $p < 0.05$ (*), $p < 0.01$ (**), $p < 0.001$ (***), and $p < 0.0001$ (****). Statistical analysis was performed using GraphPad Prism Software (version 9.3).

4. Conclusions

Pain is a multifaceted experience influenced by peripheral, central, immune and psychological factors. Targeting multiple pathways offers a holistic approach, improving efficacy, minimizing side effects, and reducing tolerance compared to single-target drugs. In vivo-guided approach are a promising tool for discovering multitarget analgesics. This study used this to identify a novel analgesic targeting key pathways in pain perception, transmission and regulation.

A new scaffold (**3**) inspired by the pharmacophores of opiranserin and vilazodone has been designed and the synthesized its analogs were screened for the 2nd phase inhibition in the formalin test, among which compound **29** was selected for further investigation.

In the formal model, compound **29** exhibited the high potency with an ED_{50} value of 0.78 mg/kg in the second phase with a tendency of concentration-dependent inhibition during the first phase. In the SNL neuropathic pain model, it demonstrated dose-dependent analgesic effects by increasing the withdrawal threshold with 24 and 45% MPE at 50 and 100 mg/kg, respectively. Extensive mechanism

 doi:10.20944/preprints202412.2383.v1

study indicated that it analgesic activity is primarily attributed to its strong triple uptake inhibition, particularly at DAT and SERT, along with 5-HT_{2A} antagonism.

In BBB PAMPA experiment, it showed high BBB permeability suitable for CNS drugs. The in vivo pharmacokinetics study in rats showed that ip administration provided 5-fold greater exposure and 2-fold higher stability compared to oral administration. Following ip administration, the half-life was 3.49 h with a T_{max} of 2.83 h, while po administration resulted in a half-life of 1.67 h and a T_{max} of 1.50 h. For the in vitro toxicity study, it was nontoxic to HT-22 normal neuronal cell but potential hERG inhibition with 52.7% inhibition at 10 μM. Additionally, in the CYP inhibition study, it displayed strong inhibiton of CYP3A4, while showing minimal inhibition of other tested isozymes.

Overall, compound **29** is a novel and potent analgesic identified through an in vivo-guide approach with a multarget mechanism. Further optimization is in progress to minimize the observed side effects.

Author Contributions: Conceptualization, J.L.; investigation, G.Z., N.D., N.M., H.H., He.K., Hy.K. and K.C.; writing, J.A. and J.L.; supervision, J.A. and J.L.; project administration, J.A.; funding acquisition, J.A. and J.L. All authors have read and agreed to the published version of the manuscript.

Funding: This work was supported by the National Research Foundation of Korea (NRF) grant funded by the Korea government Ministry of Science and ICT (MSIT) (No. NRF-2022R1A2C2004933 and NRF-2022R1C1C2008307).

Institutional Review Board Statement: The animal study protocol was approved by the Animal Care and Use Committee of Medifron (approval number: Formaline test: Medifron 2018-4, Chung's model: Medifron 2018-7).

Informed Consent Statement: Not applicable.

Data Availability Statement: Data is contained within the article.

Conflicts of Interest: The authors Hee-Jin Ha, Hee Kim, Hyunsoo Kim, and Kwanghyun Choi were employed by Medifron DBT. The remaining authors declare that the research was conducted in the absence of any commercial or financial relationships that could be construed as a potential conflict of interest.

References

1. Woolf, C.J. Central sensitization: Implications for the diagnosis and treatment of pain. ***Pain*** **2010**, *152*, S2-S15.
2. Basbaum, A.I.; Bautista, D.M.; Scherrer, G.; Julius, D. Cellular and molecular mechanisms of pain. ***Cell*** **2009, *139***, 267-284.
3. Borsook, D.; Hargreaves, R. Advancing pain therapeutics. ***Neuron*** **2011, *69***, 629-649.
4. Gilron, I.; Jensen T.S.; Dickenson, A.H. Combination pharmacotherapy for management of chronic pain: from bench to bedside. *Lancet Neurol*. **2013**, *12*, 1084-1095.
5. *Pang, M.H.; Kim, Y.; Jung, K.W.; Cho, S.; Lee, D.H. A series of case studies: practical methodology for identifying antinociceptive multi-target drugs. Drug Discov. Today* ***2012***, *17, 425-434.*
6. Dvoracsko, S.; Stefanucci, A.; Novellino, E.; Mollica, A. The design of multitarget ligands for chronic and neuropathic pain. *Future Med. Chem.* **2015**, *7*, 2469–2483.
7. Turnaturi, R.; Aricò, G.; Ronsisvalle, G.; Parenti, C.; Pasquinucci, L. Multitarget opioid ligands in pain relief: New players in an old game. *Eur. J. Med. Chem*. **2016**, *108*, 211-228.
8. Reichling, D.B.; Levine, J.D. Critical role of nociceptor plasticity in chronic pain. Trends *Neurosci*. 2009, *32*, 611-618.
9. Hachicha, M.; Yao, Y.; Smith, J. In vivo pharmacological models for drug discovery in pain. *Drug Discov. Today* 2015, *20*, 755-762.
10. Petersen, G.; Amrutkar, D.V. Discovery of novel analgesics using translational models of pain. *J. Transl. Med*. 2019, *17*, 86.

 doi:10.20944/preprints202412.2383.v1

11. Nedeljkovic, S.S.; Song, I.; Bao, X.; Zeballos, J. L.; Correll, D.J.; Zhang, Y.; Ledley, J.S.; Bhandari, A.; Bai, X.; Lee, S.R.; Cho, S. Exploratory study of VVZ-149, a novel analgesic molecule, in the affective component of acute postoperative pain after laparoscopic colorectal surgery. *J. Clin. Anesth.* **2022**, *76*, 110576.
12. Available online: Vilazodone (Monograph) https://www.drugs.com/monograph/vilazodone.html (accessed on 20 Dec 2024).
13. Hughes, Z.A.; Starr, K.R.; Langmead, C.J.; Hill, M.; Bartoszyk, G.D.; Hagan, J.J. et al. Neurochemical evaluation of the novel 5-HT1A receptor partial agonist/serotonin reuptake inhibitor, vilazodone. *Eur. J. Pharmacol*. **2005**, *510*, 49–57.
14. Dubuisson, D.; Dennis, S.G. The formalin test: a quantitative study of the analgesic effects of morphine, meperidine, and brain stem stimulation in rats. *Pain* 1977, *4*, 161-174.
15. Hunskaar, S.; Hole, K. The formalin test in mice: dissociation between inflammatory and non-inflammatory pain. *Pain* 1987, *30*, 103-114.
16. Shibata, M.; Ohkubo, T.; Takahashi, H.; Inoki, R. Modified formalin test: characteristic biphasic pain response. *Pain* 1989, *38*, 347-352.
17. Tjølsen, A.; Berge, O. G.; Hunskaar, S.; Rosland, J. H.; Hole, K. The formalin test: an evaluation of the method. *Pain* 1992, *51*, 5-17.
18. Coderre, T. J.; Fundytus, M. E.; McKenna, J. E.; Dalal, S.; Melzack, R. The formalin test: a validation of the weighted-scores method of behavioral pain rating. *Pain* 1993, *54*, 43-50.
19. Zhou, J.; Jiang, X.; He, S.; Jiang, H.; Feng, F.; Liu, W.; Qu, W.; Sun, H. Rational Design of multitarget-directed ligands: Strategies and emerging paradigms. *J. Med. Chem*. **2019**, *62*, 8881-8914.
20. Kim, S.H.; Chung, J. M. An experimental model for peripheral neuropathy produced by segmental spinal nerve ligation in the rat. *Pain* **1992**, *50*, 355–363.
21. Bonin, R.P.; Bories, C.; De Koninck, Y. A simplified up-down method (SUDO) for measuring mechanical nociception in rodents using von frey filaments. *Mol. Pain*, **2014**, *10*, 1744-8069-10–26.